

AD-A034 881

AIR FORCE INST OF TECH WRIGHT-PATTERSON AFB OHIO SCH--ETC F/G 9/1
THERMAL NEUTRON DAMAGE IN BIPOLAR PNP TRANSISTORS.(U)
DEC 76 T D STANLEY

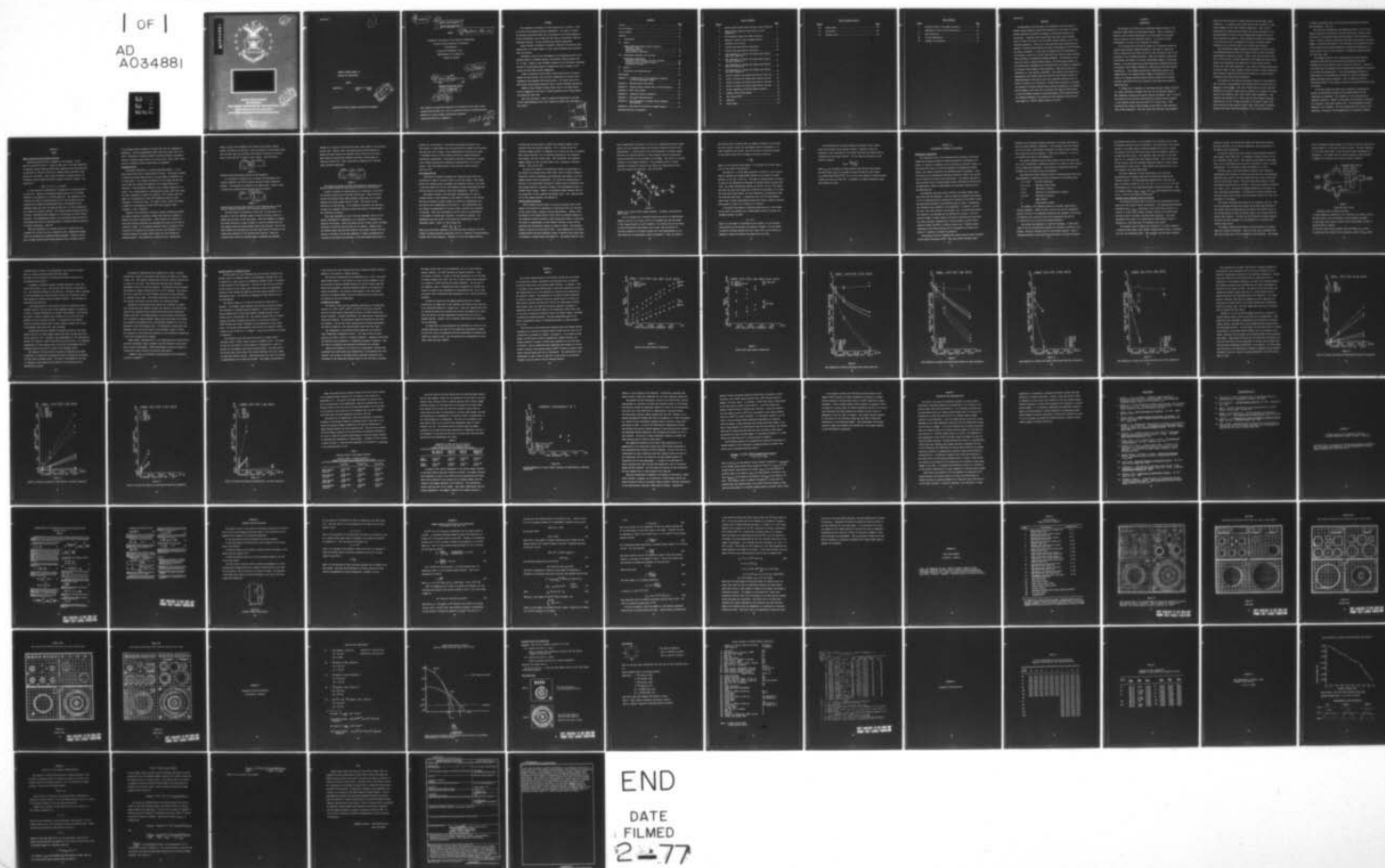
UNCLASSIFIED

ONE/PH/76-6

NL

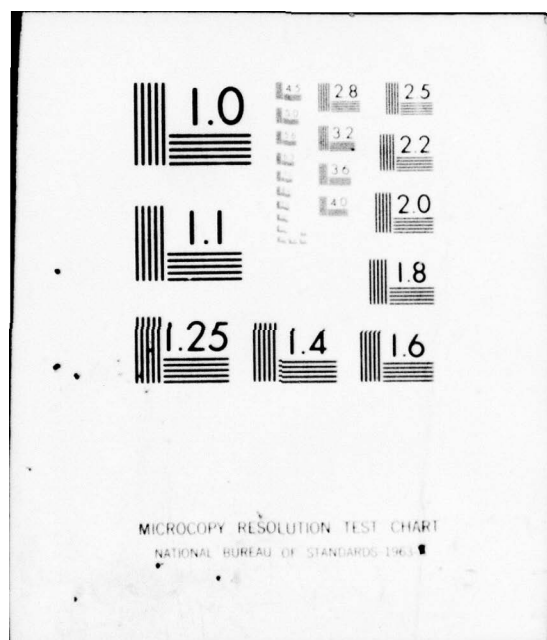
| OF |

AD
A034881

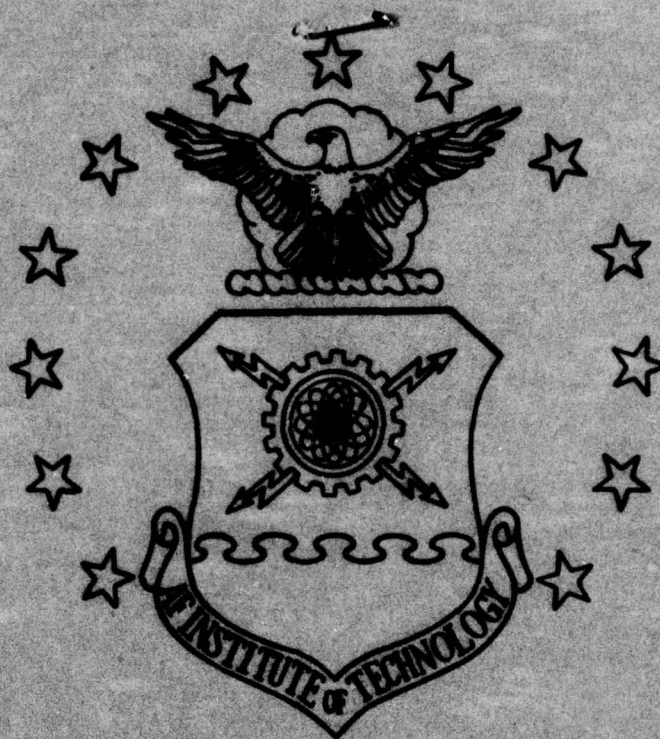


END

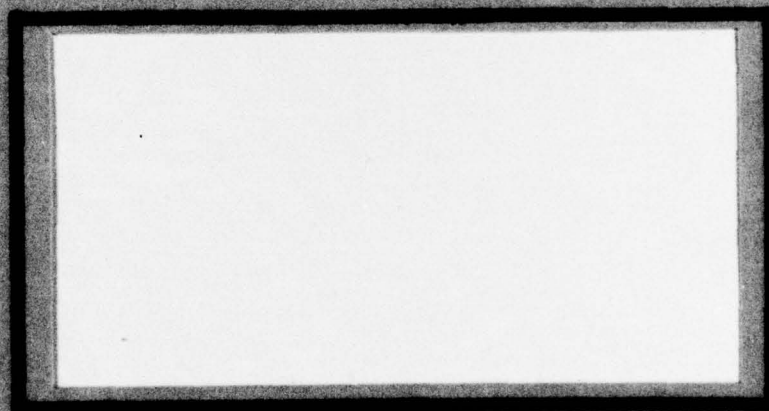
DATE
FILMED
2-77



ADA034881



(L)



UNITED STATES AIR FORCE
AIR UNIVERSITY
AIR FORCE INSTITUTE OF TECHNOLOGY
Wright-Patterson Air Force Base, Ohio

DDC
REF ID: A67127
JAN 26 1977
REGISTRY

DISTRIBUTION STATEMENT A
Approved for public release
Distribution Unlimited

GNE/PH/76-6

1

**THERMAL NEUTRON DAMAGE IN
BIPOLAR PNP TRANSISTORS**

THESIS

GNE/PH/76-6

**Timothy D. Stanley
Capt. USAF**

**DDC
RECEIVED
JAN 26 1977
AUGUST 15**

Approved for public release; distribution unlimited

(14) GNE/PH/76-6

(6) THERMAL NEUTRON DAMAGE IN
BIPOLAR PNP TRANSISTORS.

THESIS

(9) Master's thesis,

Presented to the Faculty of the School of Engineering
of the Air Force Institute of Technology
Air University
in Partial Fulfillment of the
Requirements for the Degree of
Master of Science

(10) by
Timothy D. Stanley, B.S., M.S.
Capt USAF

Graduate Engineering Physics

(11) December 1976

(12) 88p.

(16) ADQ9

(17) 11

This research was partially supported by the Defense Nuclear Agency under
subtask Z-99Q AX TB037 work unit 01, Radiation effects on Microelectronics.
Approved for public release; distribution unlimited.
Copyrighted Material in Appendix A.

1473
012 225
SB

Preface

The originator and sponsor for this project was Dr. Patrick J. Vail of the Air Force Weapons Laboratory (AFWL/ELPT). His effort in having the required transistors made, and in arranging for the funds required to do the irradiations, and in doing the fast neutron irradiations, made the experiment possible. He also provided many helpful suggestions.

Special thanks is extended to Richard E. Anderson, who made the transistors used in a limited amount of time, and who answered many questions about the devices.

Gratitude is also due all the members of the operations staff of the National Bureau of Standards Reactor; particularly, Nathan Bickford and Dr. T. Raby. Thanks is also extended to members of the Electronic Technology Division of the National Bureau of Standards for their interest in the project and their many helpful suggestions.

A debt of gratitude is also owed to Major Bruce Pierce, my faculty advisor for this project, for his help in organizing the project and in teaching me the necessary solid state physics. Dr. George John of the AFIT faculty also provided essential help in several problems encountered.

Thanks is also extended to Major Robert Couch of the AFIT faculty for his suggestion to use Boron 11 doped transistors and to Diana Hudson for typing the final copy.

Last, but not least, I want to express my appreciation to my wife for her understanding and for proof reading and typing the rough draft of this report.

ACQUISITION	White Section	<input checked="" type="checkbox"/>
HTIS	Ref Section	<input type="checkbox"/>
INDEXED		<input type="checkbox"/>
JUSTIFICATION		
BY	DISTRIBUTION/AVAILABILITY CODES	
Dist.	AVAIL. CODE/STANDARD	
A		

Contents

	<u>Page</u>
Preface	ii
List of Figures	iv
List of Tables	vi
Abstract	vii
I. Introduction	1
II. Theory	4
Damage Producing Thermal Neutron Reactions	
Transistor Theory	5
Bulk Damage Effects	8
Lattice Defect Production	9
III. Experimental Equipment and Procedure	13
Experimental Transistors	
Transistor Test Equipment and Test Procedure	15
National Bureau of Standards Reactor	20
Irradiation Procedure	21
IV. Results	23
V. Conclusions and Recommendations	41
Bibliography	43
Appendix A: A General Proof of the Degradation Equation for Bulk Displacement Damage	45
Appendix B: Geometry Factor Calculation	48
Appendix C: Thermal Neutron Reaction Rate in PNP Transistors . .	50
Appendix D: NBS-2 Test Pattern	55
Appendix E: Transistor Process Information	62
Appendix F: Transistor Characteristics	69
Appendix G: Flux Information on Thermal Column Pneumatic Tube Facility	72
Appendix H: Derivation of the Relative Damage Equation	74
Copyright Material in Appendix A	

List of Figures

<u>Figure</u>		<u>Page</u>
1	Forward Biased Emitter-Base Junction in PNP Transistor .	6
2	Reverse Biased Collector-Base Junction in PNP Transistors	6
3	PNP Transistor Biased for Normal Operation	7
4	Example of Crystal Lattice Damage Cascades	10
5	Transistor Test Circuit	17
6	Initial Gain Small Emitter Transistors	24
7	Initial Gain Large Emitter Transistors	25
8	Gain Remaining vs. Fluence and Doping Small Emitter, High Gain Transistors	26
9	Gain Remaining vs. Fluence and Doping Small Emitter Low Gain Transistors	27
10	Gain Remaining vs. Fluence and Doping Large Emitter High Gain Transistors	28
11	Gain Remaining vs. Fluence and Doping Large Emitter Low Gain Transistors	29
12	$\Delta(1/\beta)$ vs Fluence and Doping Small Emitter High Gain . .	31
13	$\Delta(1/\beta)$ vs Fluence and Doping Small Emitter Low Gain . .	32
14	$\Delta(1/\beta)$ vs Fluence and Doping Large Emitter High Gain . .	33
15	$\Delta(1/\beta)$ vs Fluence and Doping Large Emitter Low Gain . .	34
16	Current Dependence of Various Damage Constants	37
B1	Geometry Factor Relationships	48
D1	Test Pattern NBS-2	57
D2	Base Mask	58
D3	Emitter Mask	59

List of Figures (con't)

<u>Figure</u>		<u>Page</u>
D4	Contact Mask	60
D5	Metal Mask	61
E1	Doping Profile	64

List of Tables

<u>Table</u>		<u>Page</u>
1	Relative Values of the Damage Constants	35
2	Comparison of High and Low Gain Devices	36
D1	Test Structures	56
F1	DC Gain Measurements	70
F2	Leakage for Transistors	71

Abstract

An experimental test was made of the hypothesis that the source of thermal neutron damage in bipolar PNP transistors is the result of thermal neutron captures by the Boron 10 present in the emitter region of the transistors. Transistors were specifically made using three different ratios of Boron 10 to Boron 11 as the emitter dopant material, and in four different geometries. Forty-two of these specially made transistors were exposed to thermal neutron fluences as high as approximately 5×10^{15} neutrons per square centimeter. In each case the damage observed corresponded to the fraction of Boron 10 to total boron used as the emitter dopant material, thus confirming the hypothesized damage mechanism. The dependence of the collector current, thermal neutron fluence, and emitter-base geometry on the observed gain degradation also indicated that bulk damage is responsible for thermal neutron damage in PNP transistors. Some devices were also irradiated in a fast neutron environment. Fast neutrons were found to be approximately one hundred times more effective than thermal neutrons in producing damage in the devices that use a naturally occurring ratio of Boron 10 to Boron 11 in the emitter. Formulas were developed to calculate the fraction of lithium atoms and alpha particles generated in the emitter that do damage in the base, and to calculate the relative effectiveness of fast and thermal neutrons in producing damage in PNP transistors where the combined thickness of the emitter and base regions is less than the path length of a .88 MeV lithium nucleus in silicon.

CHAPTER I

INTRODUCTION

The detonation of nuclear and thermonuclear weapons results in the release of large numbers of high-energy neutrons. When a transistor is exposed to fast neutrons, displacement of silicon atoms in the crystal lattice structure of the transistor results. As a result of these displacements, the gain of the transistor is reduced.

If in traveling from the nuclear weapon to an electronic system the neutrons pass through a moderating material like water or carbon they will be slowed down until their velocity is about the same as that of the molecules of the surrounding material. These slow neutrons, called thermal neutrons, are unable to do direct displacement damage in transistors. However, it has been observed that some transistors irradiated with thermal neutrons suffer damage comparable to that resulting from fast neutron irradiations. Since thermal neutrons have insufficient energy to do damage directly, the thermal neutron damage is hypothesized to be the result of an energy producing nuclear reaction induced by the thermal neutrons, specifically the (n, α) reaction in the boron used as emitter dopant material.

I. Arimura and C. Rosenberg of the Boeing Aerospace Company indicated in a paper published in December 1973 that they had observed damage in PNP transistors resulting from thermal neutron irradiation. (Ref. 1:274-279) They found that the relative effectiveness of thermal neutrons compared to fast neutrons varied from less than 10^{-3} to nearly unity. They discovered that thermal neutron damage was much less in NPN transistors than in PNP transistors. They also found that thin-base, high-frequency

devices are more sensitive to thermal neutrons than wide-base, power-transistors. In contrast, power transistors are more sensitive to fast neutron damage than are high frequency transistors. (Ref. 18:451). Additionally the thermal neutron fluence and current dependence of the gain degradation indicated that bulk displacement damage was the most likely degradation mechanism. These findings led Arimura and Rosenberg to the conclusion that the damage was the result of thermal neutron absorption by the Boron-10 atoms in the emitter dopant material.

This hypothesized damage mechanism is consistent with what Arimura and Rosenberg observed and has been observed also by several subsequent investigators including the author. Namely, since PNP transistors have 10^2 to 10^4 more boron than NPN transistors, PNP transistors should suffer greater gain degradation when subjected to a given thermal neutron fluence than should NPN transistors. Also, since the doping concentration is usually higher in high frequency transistors than in power transistors, high frequency transistors should be more sensitive to thermal neutron irradiation than should power transistors.

The fraction of the atoms in the emitter region of a PNP transistor that are boron is approximately one thousandth and the fraction that are Boron 10 is about 0.0002. Also, only a small fraction of the particles produced in the emitter region would be expected to do damage in the base region of the transistor that could result in gain degradation. Some tentative calculations by Dr. Vail of the Air Force Weapons Laboratory indicated that as few as twenty reactions in the emitter region could have occurred for some reported fluence levels using typical transistor geometry and doping level (see Appendix C for Dr. Vails Calculation).

It seems inconceivable that so few particles could produce observable gain degradation. (Ref. 19)

The Electronic Phenomenology and Technology Branch of the Air Force Weapons Laboratory, Kirtland Air Force Base, New Mexico, needed to know the source of the observed thermal neutron damage in PNP transistors in order to develop a means of performing theoretical calculations of expected damage in radiation environments. For this reason they proposed the study of the thermal neutron damage mechanism in bipolar PNP transistors as a thesis topic at the Air Force Institute of Technology, Wright-Patterson Air Force Base, Ohio.

The approach chosen for the investigation was to have some PNP transistors made that were electrically and physically identical, differing only in the isotopic ratio of Boron-10 to Boron-11. These devices would then be irradiated and the observed gain degradation correlated to the Boron-10 concentration. If the gain degradation observed is proportional to the concentration of Boron-10, then the hypothesized damage mechanism would be supported. Also, by having the devices specifically made for this purpose, control over the device geometry would be possible.

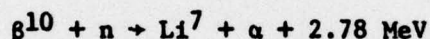
In the next chapter the basic theory required to understand and analyze the hypothesized thermal neutron damage mechanism in PNP transistors are presented. Also included is a short description of transistor operation. Chapter III describes the transistors, transistor test equipment, and nuclear reactors used. The experimental procedure employed is also included. The final chapters give the results of the experiment, conclusions, and recommendations for additional research.

CHAPTER II

THEORY

Damage Producing Thermal Neutron Reactions

Naturally-occurring boron is composed of two isotopes: 19.78% Boron-10 and 80.22% Boron-11. Boron-10 atoms have a very high probability of capturing thermal neutrons (3840 barns) compared to most materials and in particular to Boron-11, which has a thermal neutron activation cross section of 0.005 barns. When a Boron-10 absorbs a thermal neutron, an exothermic reaction takes place which releases 2.78 MeV of energy. The reaction is:



In this reaction the probability of forming Li^7 in the ground state is only 6.4%. Usually an intermediate excited state of Li^7 is formed followed by the emission of a 0.48 MeV gamma ray. The remainder of the 2.78 MeV (2.30 MeV) is divided between the Li^7 and the alpha particle. Conservation of momentum considerations lead to the division of the remaining energy such that the alpha particle has 1.47 MeV of energy and the lithium ion receives 0.88 MeV. The lithium nucleus and alpha particle fly apart, dissipating their energies in a few microns of crystal lattice structure. The displacements caused by the lithium and alpha recoils are the hypothesized source of gain degradation in thermal neutron irradiation of bipolar transistors. (Ref 19)

Since the absorption of a thermal neutron by a silicon atom can transmute the silicon atom into a phosphorus atom, transmutation-doping has to be considered as a possible damage mechanism. However, silicon has a thermal neutron capture cross section of only .09 barns; and out

of one hundred neutron captures in silicon only four are transmuted to phosphorus. Also the transmutation takes place with a half life of 2.6 hours. Absorption of thermal neutrons by silicon produces an average of 780 MeV of kinetic energy applied to a silicon atom. (Ref. 5:391) Thus, while not promising, silicon capture must be considered.

Transistor Theory

The bipolar transistor is a current amplifying device. It is a three-region device and is usually made of silicon. The regions are made by doping the silicon with boron for a p-type region or phosphorus for a n-type region. In p regions the majority of the charge carriers are holes, while in n regions the majority of the charge carriers are electrons. A PNP transistor consists of two p regions separated by a n region. One P region doped to a concentration of about 10^{16} boron atoms per cubic centimeter is called the collector. The N region, which is doped to a concentration of about 10^{18} phosphorus atoms per cubic centimeter, is called the base. The final P region, called the emitter, is doped to a concentration of about 10^{20} boron atoms per cubic centimeter. (Ref. 3:201-204).

Because of the difference in majority carrier concentration across the region boundaries, diffusion currents will flow in an attempt to balance the carrier concentrations. These currents will continue to flow until internal potentials are developed that cause the net flow of carriers to cease. If an external potential source is supplied to the junction of two regions with polarity such that the formation of an internal potential is opposed, then current will flow through the potential source. This condition is referred to as a forward bias.

Figure 1 shows a PNP transistor with forward bias potential applied between the emitter and the base. Since the emitter is more heavily doped than the base, most of the current flow across the junction is from the flow of holes from the P region to the N region. (Ref 12:432-433)

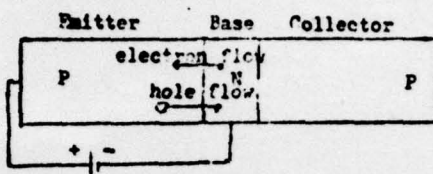


Figure 1

Forward Biased Emitter-Base Junction in PNP Transistor

If a potential is applied so as to enhance the development of an internal potential, the flow of charge carriers is almost completely stopped. This situation is referred to as reverse bias. Figure 2 shows a reverse bias applied between the base and the collector.

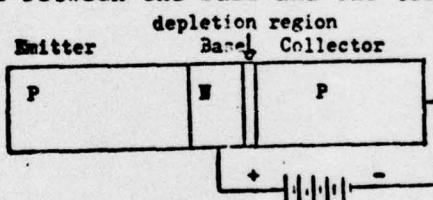


Figure 2

Reverse Biased Collector-Base Junction in PNP Transistor: only the few carriers thermally generated in the depletion region will flow.

The base region in transistors is very thin, (on the order of .5 microns) so that the diffusion length of minority carriers, holes, is longer than the width of the base region. When the transistor is biased for normal operation as shown in Figure 3, holes are injected into the base region across the forward biased emitter base junction. Most of the holes diffuse right through the thin base region and are collected in the reverse bias potential of the collector base junction. Since the collector-base junction is reverse biased, increasing the potential

between the collector and the base will have little effect on the collector current flow. However, since the forward bias potential between the emitter and base controls the diffusion flow of holes into the base, a small change in emitter-base potential can cause a large change in collector current flow. Thus a power gain in signals can be achieved using transistor amplifiers.

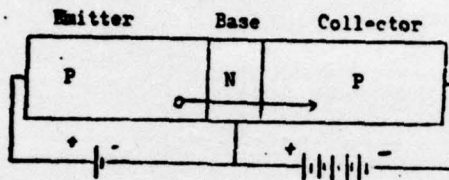


Figure 3

PNP Transistor Biased for Normal Operation: holes generated in the emitter diffuse through the base and are collected in the collector.

DC gain, a measure of relative merit of a transistor, is the ratio of collector current flow to the base current flow. Ideally the base current flow should be very small, giving a large gain, but in actual practice the DC gain ranges from 20 to 1000. The DC gain is also referred to as Beta and H_{FE} . To be completely specified, the gain must be given for a specific collector current and specific voltage between the collector and emitter.

Since gain degradation is one of the most important effects of the neutron irradiation of transistors, it is important to understand the origin of the DC gain. There are several sources of base current including injection of electrons from the base into the emitter, leakage across the reverse biased collector-base junction, and surface currents from the emitter to the base, but the main component is usually recombination of a portion of the holes with electrons in the base region before they can

diffuse into the collector. Since holes are minority carriers in the base region, it seems likely that the holes would all combine with electrons. This does not occur, however, since recombination of electrons and holes is forbidden except at lattice defect sites due to quantum mechanical conservation requirements. These defect sites may be impurities or energy level changes resulting from vacancies or interstitials in the crystal lattice. Many such defects exist in even the best silicon crystals.

(Ref 10:11-13)

Bulk Damage Effects

Fast-neutron irradiation degrades the transistor gain directly by increasing the number of lattice defects in the base region. Even though defects are produced evenly throughout the transistor material, only those in the base region (and the two thin-depletion regions separating the base from the emitter and collector) cause gain degradation. (Ref 8:27)

The minority carrier life time before recombination of a hole in N-doped silicon is thus dependent on the number of defects in the silicon. One over the minority carrier lifetime is called the recombination rate per carrier and is symbolized by the letter R. The recombination rate per carrier is proportional to the base current and hence the reciprocal of the gain. Also, the recombination rate per carrier is proportional to the number of defects and, therefore, the radiation exposure. Recombination rate per carrier is the sum of the recombination rates of different origins. Hence, it can be shown that

$$\Delta(1/\beta) = \frac{1}{\beta_f} - \frac{1}{\beta_1} = C\phi$$

where β_f is gain after exposure, β_1 is the gain before exposure, ϕ is the fluence of damage producing radiations, and C is a constant of proportionality. Another form of this equation, referred to as the bulk damage equation,

has been used for many years to predict the expected change in gain resulting from fast neutrons exposure. The C , usually called the radiation damage constant, is dependent on the energy and type of displacement causing radiation, and the physical properties of the transistor, most notably, the base transit time. (Ref 10:160-168) The radiation damage constant (C) has also been shown to be a function of collector current. (Ref 17:310, 316)

As long as the number of recombination centers is proportional to the fluence of radiation and no other effect (such as surface leakage or mechanical failure) predominates and significant gain remains, the bulk damage equation should be applicable. As long as the concentration of Boron-10 is not appreciably decreased by thermal neutron irradiation, the bulk damage equation is expected to apply to the hypothesized source of thermal neutron damage. However, the radiation damage constant would be very sensitive to device geometry and doping levels. For a general proof of the bulk damage equation, see Appendix A.

Lattice Defect Production

When a charged particle moves in a lattice structure, most of the energy of the particle is dissipated in interactions with the electrons of the lattice atoms, causing no lattice displacements. However, when the energy of the charged particle falls below the threshold energy for the particular lattice structure, atomic interactions begin to take place. The result is displacement of atoms leaving vacancies in some lattice positions and interstitials (excess of atoms) in others. The threshold energy in silicon is 145 KeV (Ref 6:445). Atoms displaced by the initial charged particle may have sufficient energy to displace other atoms thereby producing a cascade effect (see Figure 4). The energy required to pro-

duce a displacement in silicon is 12.9 eV, so a charged particle with energy greater than the threshold energy could produce a maximum of about 11,000 displacements. A large portion of the atoms displaced in radiation damage move back into lattice positions or form complexes (such as divacancies) within milliseconds of the occurrence of the damage. The result is a partial "healing" of the damaged transistor. This phenomenon which is called annealing is temperature sensitive; the higher the temperature the more rapid and complete the annealing. (Ref 10:197-198)

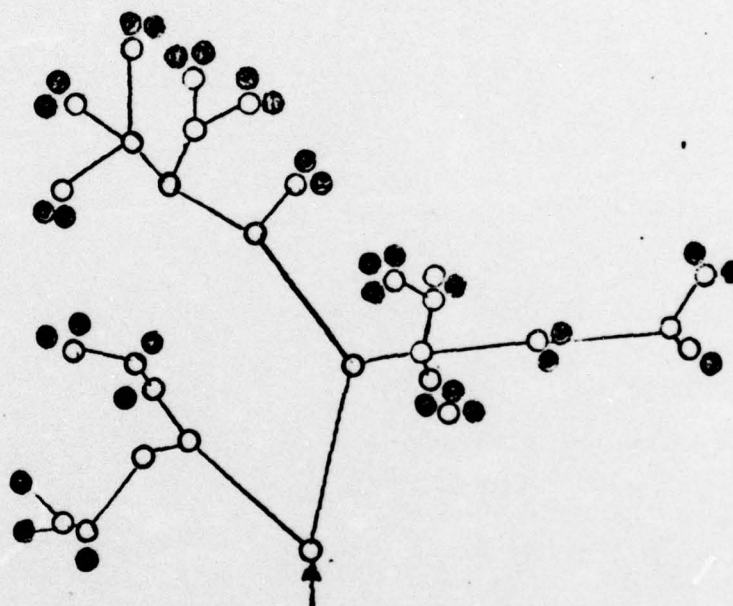


Figure 4

Example of a crystal lattice damage cascades. \circ vacancy, \bullet interstitials (Ref. 11:26)

If it is assumed that a charged particle does all of its displacement damage at the end of its path, and if it is assumed that the path length of the charged particle is small compared to the surface area of the device so that semi-infinite slab geometry can be used, then the portion of particles produced in the emitter region that cause displacements in the base region can be calculated as shown in Appendix B. Also, the range of

the particle must be greater than the combined thickness of the emitter and base regions to apply the relationship derived in Appendix B. If these assumptions can be made, then the fraction of particles produced in the emitter region that do damage in the base is given by

$$G = \frac{h}{2R}$$

where G is the fraction doing damage, h is the width of the base region, and R is the range of the particle.

The range of a 1.47 MeV alpha particle in silicon is 5.5 μ m as determined by applying the Bragg-Kleeman equation to the range of an alpha particle in air (Ref. 15:10, 11). The range of lithium nuclei in silicon is given in ion implantation literature for various initial energies (Ref 7:26). By linear interpolation between the 300 keV and the 1 MeV ranges, one finds the total path length for a 0.88 MeV Li in silicon to be 3.12 μ m. The total path length should, for this application, be corrected to give the projected path length. A correction factor of 0.96 was obtained, again using a linear interpolation between data points, giving a projected path length of 3.00 μ m for a 0.88 MeV Li in silicon.

To calculate the number of reactions taking place in a unit volume as the result of irradiation by a monoenergetic source of neutrons the following equation is used:

$$R = \sigma N \phi$$

where R is the number of reactions per unit volume, σ is the reaction cross section for the reaction and energy of interest, N is the number of atoms of reacting material per unit volume, and ϕ is the fluence of neutrons to which the material was exposed per unit area.

For distributions of neutron energies the problem is more complex since cross sections are functions of energy. Appendix C shows the derivation of the reactions per unit volume resulting from thermal neutron irradiation of boron doped silicon. For this case the reaction per unit volume is given by

$$R_{\alpha, Li} = \frac{N_{B10} \sigma_o \phi}{1.128}$$

where $R_{\alpha, Li}$ is the number of alpha particles and lithium atoms produced per unit volume, N_{B10} is the number of Boron 10 atoms per unit volume, σ_o is 3840 barns = $3.84 \times 10^{-21} \text{cm}^2$, and ϕ is the total number of thermal neutrons incident per unit area (Ref 19). In Appendix C a sample calculation using this equation is given.

CHAPTER III

EXPERIMENTAL EQUIPMENT AND PROCEDURE

EXPERIMENTAL TRANSISTORS

The transistors used in this experiment were produced at the Device Design and Processing Division of Sandia Laboratories, Albuquerque, New Mexico, by Richard E. Anderson under the direction of William R. Dawes, Jr. The devices were made in an Extrion Automated Ion-implantation Chamber using a test pattern produced by the National Bureau of Standards. Since the process of ion-implantation separates isotopes by weight, the isotopic ratio of Boron-10 to Boron-11 was controllable. The devices were made in three isotopic ratios of emitter-dopant atoms; 100% Boron-10, 20% Boron-10 and 80% Boron-11 (which is approximately the naturally occurring ratio), and 100% Boron-11.

Two different times were used to drive-in the emitter dopant atoms after they were ion implanted. Since the base had previously been driven-in for an extended period of time only the thickness of the emitter region was appreciably affected by the different drive-in times. Consequently, the transistors were available in two geometries: 1) emitter $1.1\mu\text{m}$ and the base $.5\mu\text{m}$, and 2) emitter $.9\mu\text{m}$ and base $.7\mu\text{m}$. The narrow-base devices are referred to as high-gain and the wide-base as low-gain. For both cases the number of dopant atoms in the emitter region was the same since the boron atoms were implanted with a surface density of 5×10^{15} boron atoms per square centimeter of emitter surface area. Complete process information with doping profiles and pin arrangement as received from Richard E. Anderson is included in Appendix D.

The National Bureau of Standards test pattern used was NBS-2 described in NBS Special Publication 400-6. This test pattern includes twenty

different test structures including capacitors, resistors, and diodes as well as several different transistors. The structures that were "bonded out" for use were a small emitter transistor, an emitter sheet resistor, and a large area tetrode transistor. These are structures 7, 15, and 19 on the NBS-2 test pattern (see Appendix E).

The tetrode transistor has two base contacts, one at the center and one at the circumference, enabling the device to be used as a base resistor or as a large area transistor. Since there is no passivation mask with the NBS-2 set, the devices were not passivated.

Thus there were twelve different types of transistors made which were distinguished by a number and a letter according to the following code:

2, 6, or 10	Low Gain (wide base)
4, 8, or 12	High Gain (narrow base)
2 or 4	100% Boron 11 emitter
6 or 8	20% Boron 10 and 80% Boron 11 emitter
10 or 12	100% Boron 10 emitter
A	Small emitter
B	Large emitter tetrode

For example, a 2B transistor would be a low gain, 100% Boron-11 tetrode transistor. Twelve of each of the 4A, 8A, and 12A transistors and four of each of the remaining transistors were supplied to the author. An additional set of three of each of the transistors was sent to Dr. Patrick Vail of the Air Force Weapons Laboratory.

The devices were supplied in 8 lead TO-5 packages. A field plate contact over the collector-base junction was included in addition to the emitter, collector, and base (two for the tetrode) contacts. Since a changing potential on the field plate could affect the device operation

and radiation sensitivity, it was soldered to the collector lead so that a consistent potential would be maintained. The leads going to the emitter resistor in the small emitter transistor package were bent 90° forward and spaced so that they could make contact with four adjacent contacts in an eight lead TO-5 socket. The transistor leads were bent so that they would fit in a standard four lead transistor socket. Each of the devices of each specific type were assigned consecutive numbers to enable unique identification of each device. These numbers were painted on the top of the transistor case with enamel paint.

The three transistors of each variety sent to Dr. Vail were characterized on the Weapon Laboratory's Fairchild 600 Computerized Transistor Testor. The characteristics measured by Dr. Vail were the gain at collector currents of .01, .02, .05, .1, .2, .5, 1, 2, 5, 10, and 20 milliamps with 5 volts maintained between collector and emitter. Also the leakage currents $I_{(CBO)}$, $I_{(EBO)}$, and $I_{(CEO)}$ were measured with voltages of 10, 3, and 10 Volts applied respectively.

Transistor Test Equipment and Test Procedure

The seventy-two devices sent to the author were characterized by him before and after thermal neutron irradiations. The characteristics measured included DC gain, $I_{(EBO)}$, capacitance of the emitter-base junction as a function of reverse bias voltage, breakdown voltage of the emitter-base junction, emitter resistance, and base sheet resistance. Also scope photographs were taken of the common emitter characteristic curves as displayed on a Tektronik Type 575 Transistor Curve Tracer.

The equipment used to measure gain consisted of a current regulator, a regulated power supply, three digital voltage-current meters, a transistor test box, and connecting cables. This equipment was also used to measure

saturation voltage, the voltage drop across the emitter base junction, the base resistance for the tetrode transistors, and the resistance of the emitter sheet resistances.

The current regulator was built using a Kepco Operational Amplifier power supply, model OPS100-2TA. It supplied a constant current for use as a collector current source. The current was selectable in two ranges, from .25 to 10 milliamps and was set with a precision, 10 turn, 1 kilohm potentiometer. The compliance voltage was limited to 15 volts.

The base current source was formed by placing a high resistance (approximately 100 kilohms) in series with the output of a well-regulated laboratory power supply. The power supply used was a Trygon Electronics Dual Lab Power Supply, DL40-1. The power supply had an output voltage continuously variable from 0 to 40 volts. The series resistance consisted of a fixed, 2 watt, wire wound, 10 kilohm resistor and a precision, 10 turn, 500 kilohm potentiometer. By adjusting the series resistance and the power supply output voltage, the base current could be set from a few microamps to 4 milliamps.

The series resistances were housed in the transistor test box. This box also contained switches which enable the voltage being monitored to be switched from the voltage between the emitter and collector (V_{CE}) to the voltage between the base and emitter (V_{BE}) or the voltage across the emitter sheet resistor. The test box also contained the jacks necessary to attach the other equipment to the transistor or the emitter sheet resistor being tested.

The digital voltage-current meters used were Honeywell's Digitest, Model 333, Digital Multimeters. There are three digit instruments with full scale ranges down to 99.9 microamps or 99.9 millivolts. The maximum

error of reading on current ranges is 1.5% plus or minus one digit and on voltage ranges it is 0.5% plus or minus one digit. The input impedance on the 10 volt scale (which is the one used for gain measurements) is 100 megohms. The voltage drop for current readings is 100 millivolts. A diagram of the complete test circuit is given in Figure 5.

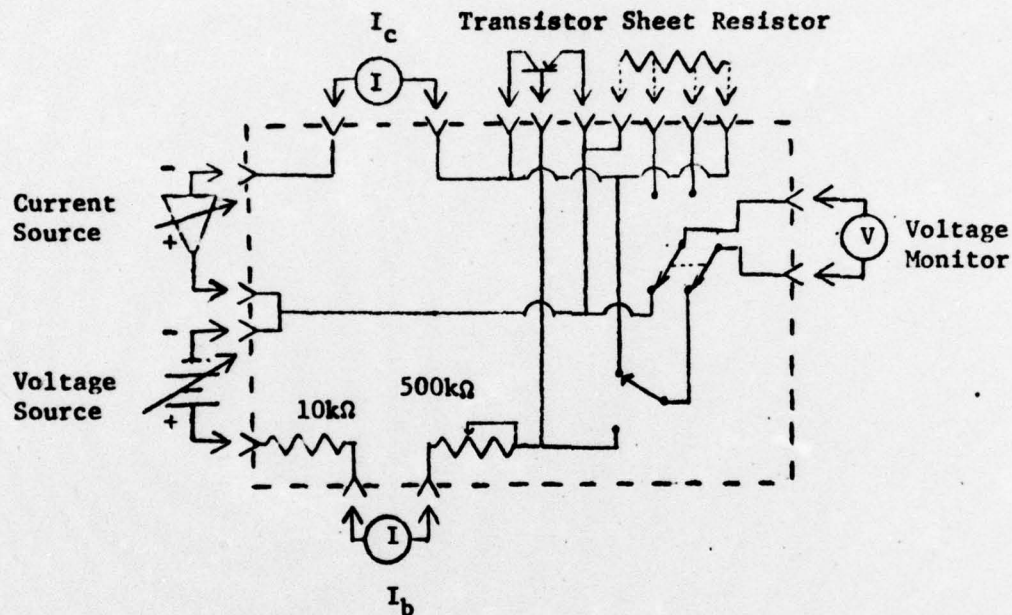


Figure 5

Transistor Test Circuit

Transistor gain is tested as follows:

- 1) After placing the transistor in the transistor test socket, turn up the base current until the reading is several hundred microamps;
- 2) then adjust the collector current source for the highest current at which the gain is desired;
- 3) then turn down the base current until the desired V_{CE} is read;
- 4) record the base current for the collector, current, and V_{CE} chosen.

5) Repeat steps 2 through 4 for successively lower collector currents until all desired operating points have been tested.

The gain is then calculated by dividing the collector current by the corresponding base current.

To measure a saturation voltage a similar procedure is used, only rather than setting a V_{CE} , a base current which results in saturation is set. The saturation voltage is read directly. The emitter sheet resistance is read by setting the collector current source for the desired current, then reading the voltage across the emitter resistor. The resistance is calculated using Ohms law.

It was observed that if the collector current is maintained over an extended period of time the gain of the transistor appears to increase as a result of thermal drifting due to internal ohmic heating. The drifting was found to cause an apparent gain increase of up to 8.5% after five minutes at 6 ma of collector current. By starting with the highest current and working quickly down to lower currents thermal drift effects are minimized, since total test time is reduced.

An additional problem, observed in measuring the gain of the large emitter devices, was large leakage current flow with the base open which was as large as 0.7 ma. Therefore, gain measurements for the large emitter devices for collector currents less than 1 ma were not used. The remaining measurements for these devices must be used with the knowledge that the indicated gain may be high as a result of the leakage current.

The leakage of the base emitter junction was measured since gamma irradiation of transistors can degrade the gain by drastically increasing the base emitter leakage current. The cause of the damage in this case is trapping of ions produced in the surface of the device above the emitter-base junction.

The method of measuring the base leakage was to apply a constant reverse bias voltage to the emitter base junction and measure the leakage current flow. The constant voltage source used was a mercury battery with an output of 1.35 volts. The current was measured using a Keithley Instruments, Model 153, Microvolt-ammeter. The Keithley Microvolt-ammeter was capable of reading currents from 10^{-1} to 10^{-11} amperes. The accuracy was plus or minus 4% on the 10^{-11} ampere scale with an input impedance of 1 megohm on that range. The battery was housed in a box with a switch that removed the battery from the circuit for zeroing the meter.

Capacitance of the emitter base junction as a function of reverse bias voltage, and the breakdown voltage, and voltage of the emitter base junction were measured using a Boonton Electronics Direct Capacitance Bridge, Model 750. The voltage applied to the transistor was monitored with a Honeywell 3-digit Voltmeter, Model 33 and the current flow through the transistor was monitored with a ME-70A/PSM-6 Standard U.S. Air Force Multimeter on the 100 microamp scale. The information obtained with this equipment, while not directly used in the experiment, helps to verify the similarity of the electrical properties of the transistors irrespective of the boron isotope used for doping.

Common emitter characteristics of the transistors were recorded before and after irradiation using a Tektronic Type 575 Transistor Curve Tracer and a Polaroid Scope Camera. These characteristic curves were taken as a backup data source and were not used as a data source.

A summary of the pre-irradiation characteristics of the transistors is given in Appendix F.

National Bureau of Standards Reactor

The NBS reactor is a D_2O moderated and cooled reactor located in the National Bureau of Standards complex at Gaithersburg, Maryland (Ref. 14). It operates at a power output of 10 megawatts (thermal) using 5.4 kilograms of fuel enriched to 93% Uranium 235. The fuel is split into two sections so that fissions are not taking place directly in front of experimental facilities thus reducing the gamma ray and fast neutron exposures in the experimental areas. The facility was designed for high thermal neutron flux experiments.

The thermal column is a 54 inch by 52 inch by 37 inch block of graphite. The thermal column pneumatic tube facility was used to expose the transistors to thermal neutron irradiation. In this facility the copper cadmium ratio is 3415 which implies a thermal neutron to fast neutron ratio of 30,000 (Ref. 16). The absolute neutron flux is 1.6×10^{11} neutrons per square centimeter per second, so that total fluences of 5×10^{15} neutrons per square centimeter can be accumulated in about eight hours. The thermal column pneumatic tube facility was carefully characterized in June of 1971 by D. A. Becker. A copy of his finding is included in Appendix G.

The transistors were sent into the reactor in a small plastic container called a rabbit, along a series of pneumatic tubes. The length of time that the rabbit is in the reactor is determined by a timer installed in the pneumatic tube facility control panel. The timer used in the control panel can be chosen from several different full scale ranges to allow more accurate setting. When setting near full scale the accuracy is approximately plus or minus two percent. The rabbits are returned to

a lead pig so that their radioactivity can be monitored without excessive exposure of the operator to gamma radiation.

Fast neutron irradiations were accomplished by Dr. Vail in the SPR-II Sandia Pulsed Reactor. This reactor is a bare critical assembly so that the spectrum of neutrons energies produced is nearly a fission spectrum. Using sulfur dosimetry a one-MeV-equivalent fluence for the neutron exposure was obtained. The relative effectiveness of fast and thermal neutrons in producing damage in the test transistors was obtained using the results of the fast irradiations.

Irradiation Procedure

One device of each type was irradiated successively to accumulative fluences of $5 \cdot 10^{11}$, $5 \cdot 10^{12}$, $5 \cdot 10^{13}$, and $2 \cdot 10^{14}$, and all but the 100% Boron-10 and 20% Boron-10 large-emitter devices to $5 \cdot 10^{14}$ neutrons per square centimeter. Between irradiations, the common emitter characteristic curves were observed. No significant change was detected for the first two fluences. For the last three fluences gain and leakage measurements were made in addition to the characteristic curves that were taken.

The temperature of the devices during irradiation was monitored using "Tempilable" Temperature Monitors. The range covered by these monitors was 130°F to 160°F in 10 degree increments. Temperature monitoring was important since annealing is a temperature dependent phenomenon. Also the times of irradiation and subsequent measurement were recorded.

Based on the finding of the first set of irradiations, fluences were calculated that would produce gain degradations of approximately 20%, 40%, and 60%. Two of each of the small-emitter high-gain transistors were irradiated to the calculated fluences except for all the Boron 11 devices.

The upper fluence limit for this experiment, set by the NBS radiation hazards committee, was 5×10^{15} neutrons per square centimeter. Since the fluence calculated to produce a 20% gain degradation in all the Boron 11 devices exceeded this limit, only two of these devices were irradiated to a fluence of 5×10^{15} neutrons per square centimeter. One of each of the remaining types of transistors was also irradiated to a fluence calculated to produce a gain degradation of approximately 60%. Due to time constraints these irradiations were performed by N.B.S. reactor operations personnel.

In order to insure that the damage observed was due to thermal neutrons and not gamma rays or fast neutrons, one device of each type was to be irradiated wrapped in a cadmium foil. Since the cadmium would block out thermal neutrons while allowing fast neutrons and gamma rays to penetrate the devices, any gain degradation observed would not be due to thermal neutrons. However, due to technical difficulties this experiment was not performed.

To insure that no stray potentials were developed as a result of the ionizing radiations, the leads of the transistors were shorted together. For the first sets of irradiations this was accomplished by inserting the leads into conductive foam. For the second set of irradiations the transistor leads were bent together.

CHAPTER IV

RESULTS

The initial characteristics of the devices confirm that the devices are electrically similar, regardless of the isotopic ratio of Boron-10 to Boron-11 atoms used as the emitter dopant material. In Figures 6 and 7 are plots of the average initial gain of the three transistors of each type characterized by Dr. Vail plotted as a function of the logarithm of the collector current. The deviations of the gains of three transistors in each set from the average for the set, varied from 4% to 12% for the small emitter devices, and from 5% to 17% for the large emitter devices. These graphs, which are taken from the data presented in Appendix F, demonstrate that the initial gains of the transistors, which differ only in the ratio of Boron-10 to Boron-11 used as the emitter dopant, correspond to within one standard deviation. The gain measurements made by the author corresponded, within 1.5 standard deviations, to those obtained by Dr. Vail.

The fraction of the initial gain remaining after each thermal neutron irradiation as a function of thermal neutron fluence for the first set of irradiations is presented in Figures 8 through 11. As is shown on these graphs the 100% Boron-10 devices degraded with roughly one-fifth the fluence required to produce a similar gain degradation in the 20% Boron-10 devices. Also no significant gain degradation was observed in the all Boron-11 devices at the maximum fluence (5×10^{14} neutrons per square centimeter) achieved during this set of irradiations. The uncertainty in the measurements of gain, which is about 5%, is the source of the apparent increase in gain in some of the all Boron-11 devices.

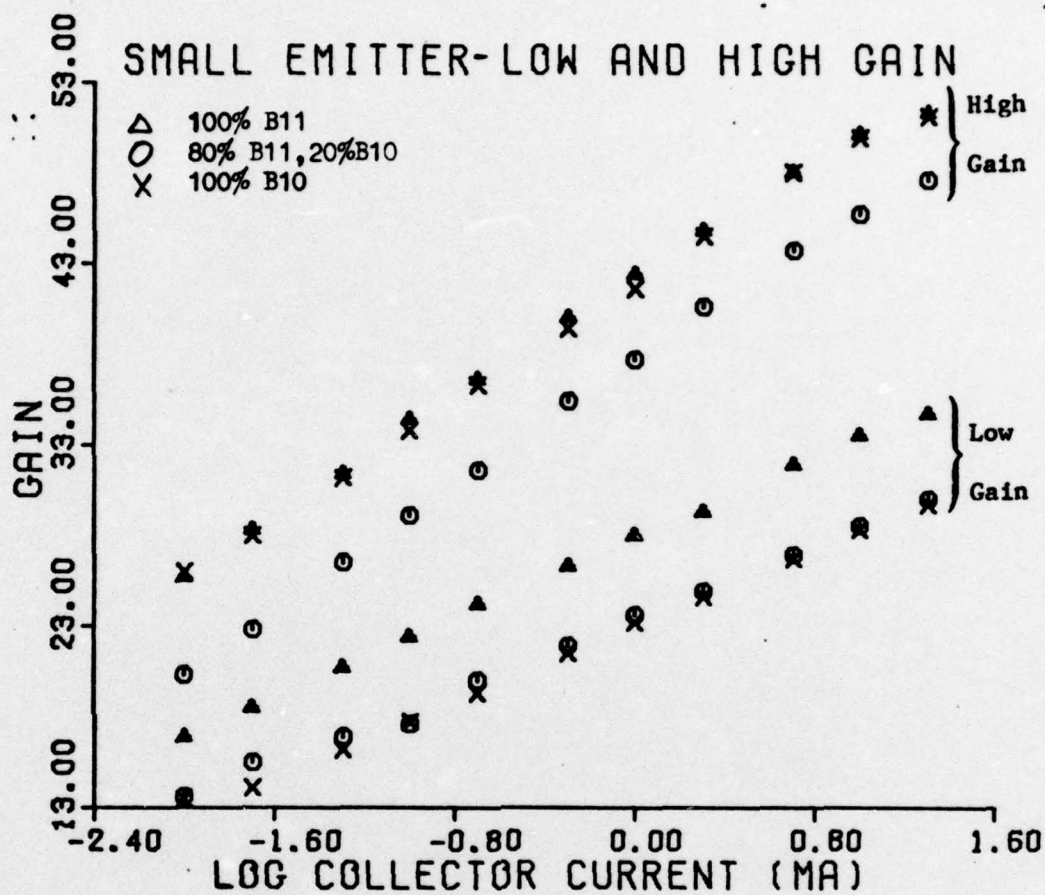


Figure 6

Initial Gain Small Emitter Transistors

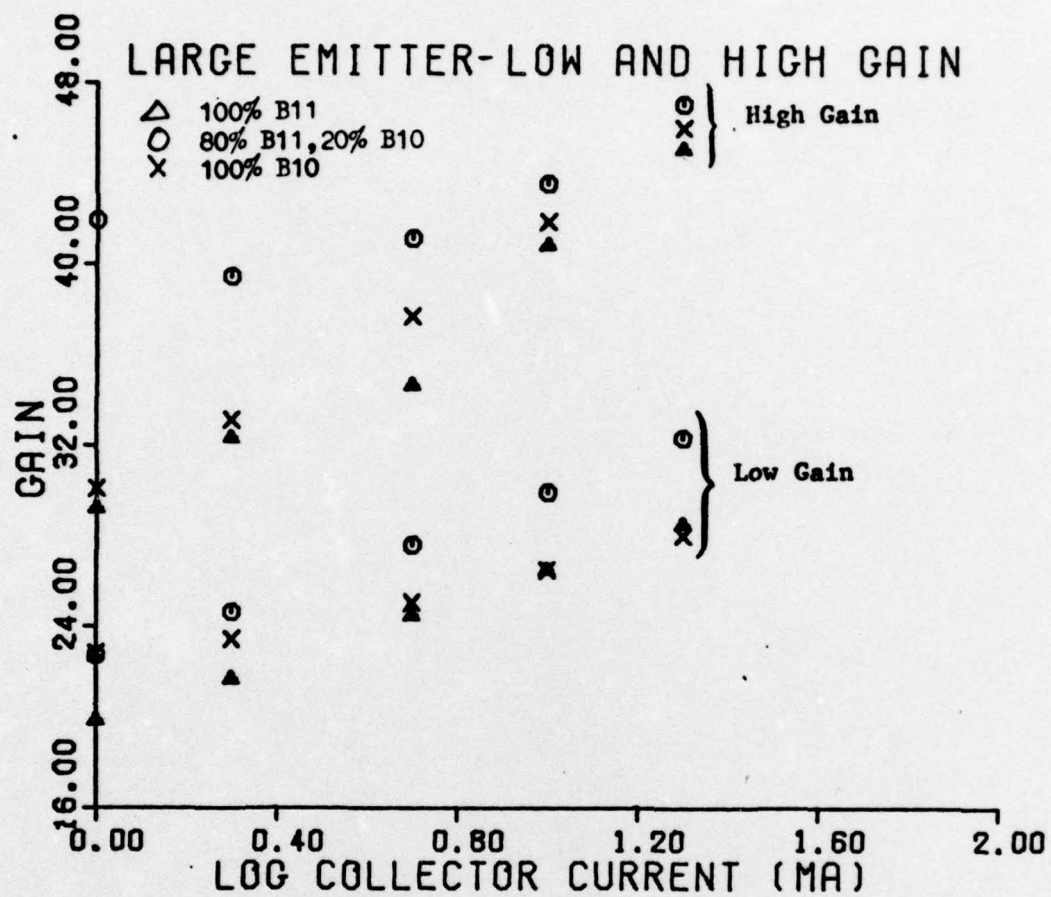


Figure 7

Initial Gain Large Emitter Transistors

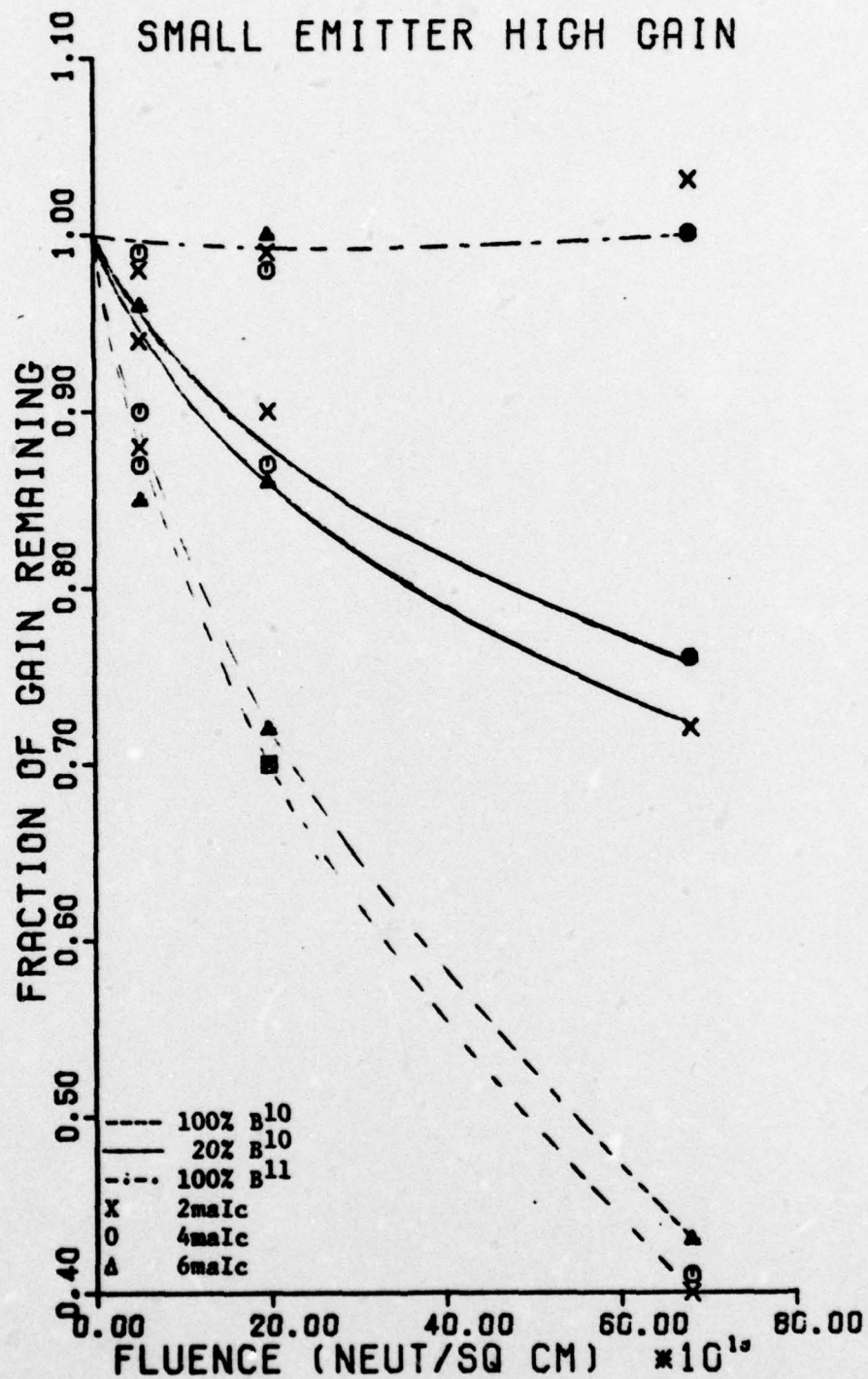


Figure 8

Gain Remaining vs Fluence and Doping Small Emitter-High Gain

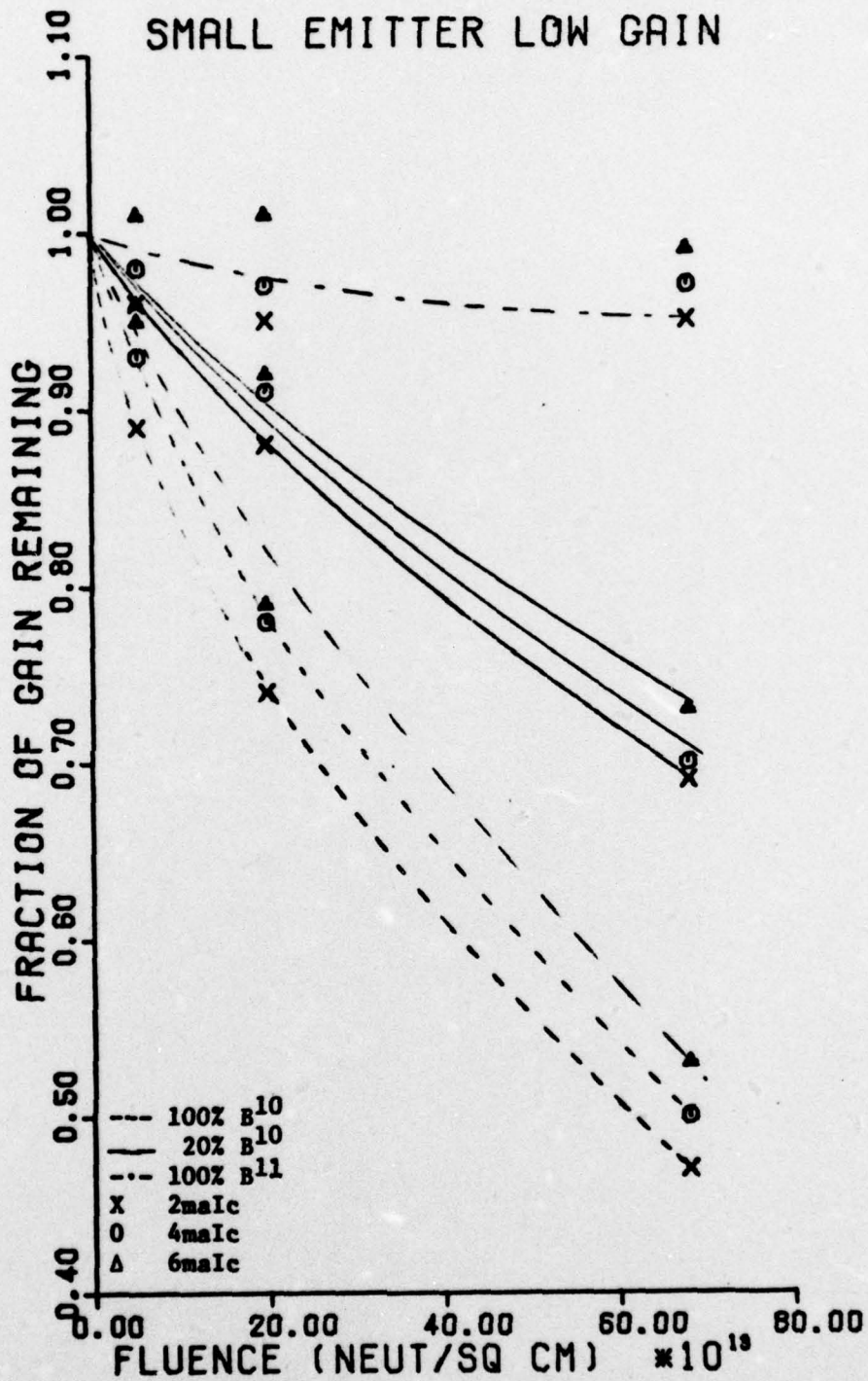


Figure 9

Gain Remaining vs Fluence and Doping Small Emitter Low Gain Transistors

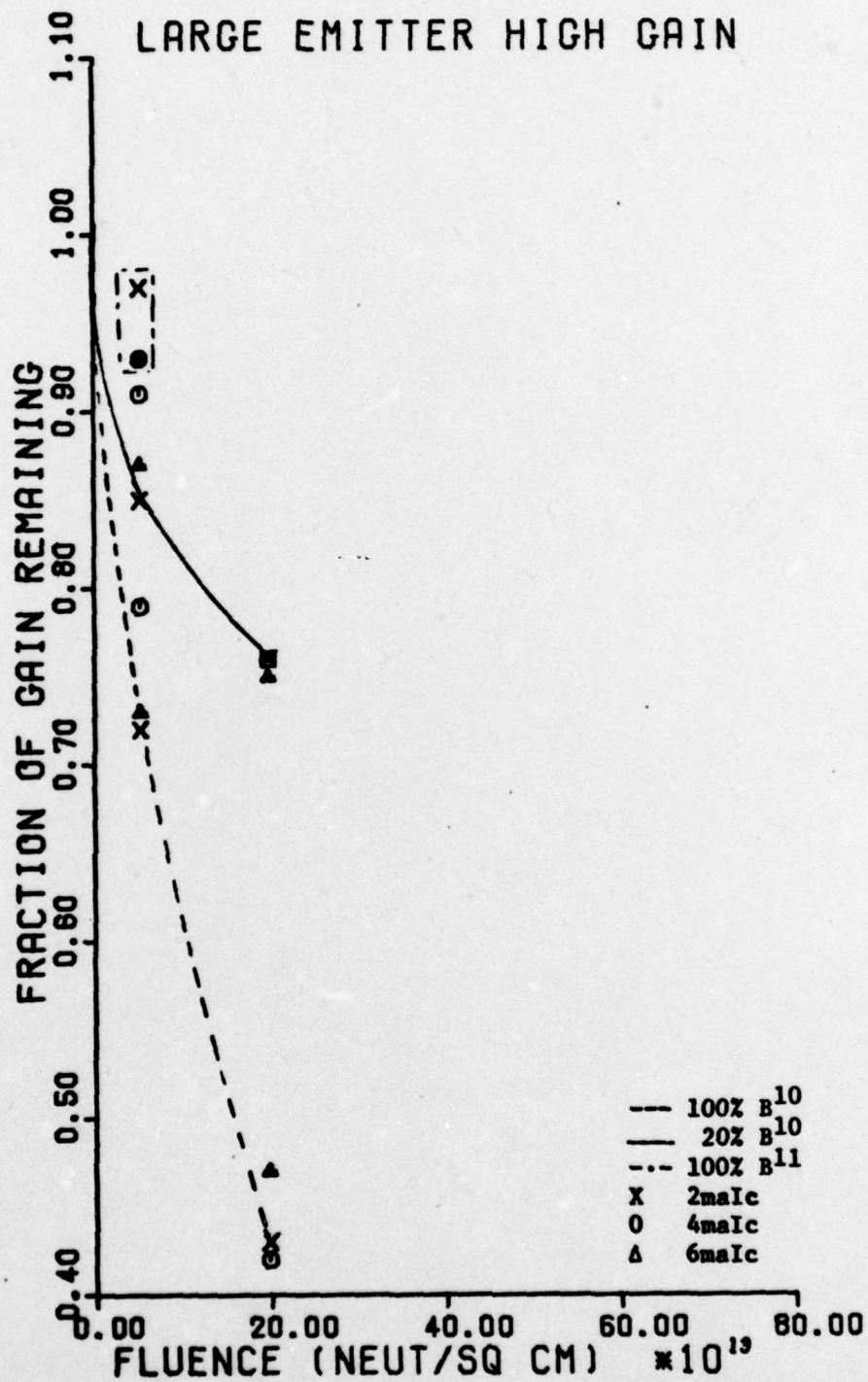


Figure 10

Gain Remaining vs Fluence and Doping Large Emitter-High Gain Transistors

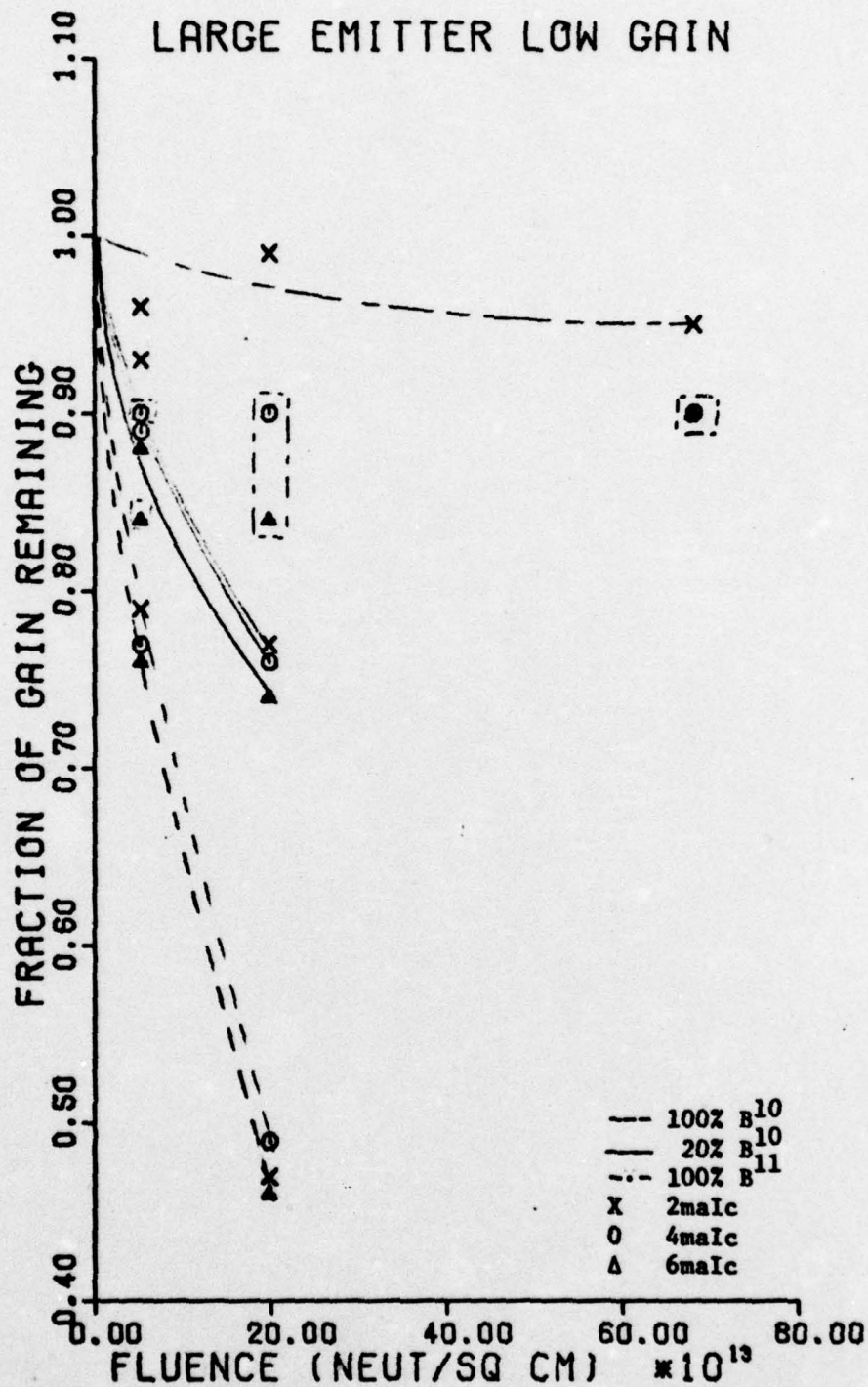


Figure 11

Gain Remaining vs Fluence and Doping Large Emitter-Low Gain Transistors

The large-emitter, low-gain, 100% Boron-11 transistor appeared to have suffered a gain degradation after its first irradiation with no additional degradation occurring for the remaining irradiations. However, since the characteristic curve photos show no change from the pre-irradiation to the maximum irradiation, and since the 2-milliamp measurement showed no change it was concluded that the initial measurement of the gain for this device was high. The source of the high initial gain reading was probably thermal drift due to a several minute delay in measuring the gain after applying power to the transistor. The large-emitter, high-gain, 100% Boron-11 transistor of this irradiation set failed due to an open circuit in the base, possibly due to mechanical shock in the rabbit tube. For this reason there was only one available data set plotted for this device.

Figures 12, 13, 14, and 15 are graphs of $\Delta(1/\beta)$ as a function of thermal neutron fluence, also for the first set of irradiations. These graphs show that the damage, as measured by the reciprocal of the gain change $[\Delta(1/\beta)]$, resulting from a given thermal neutron fluence, follows the bulk damage equation. In other words, the fact that $\Delta(1/\beta)$ is linearly proportional to the thermal neutron fluence, with the intercept at the origin, indicates that the source of the observed damage is bulk displacement damage. These graphs also show that the wider base transistors (i.e. those with Low-Gain) are more susceptible to thermal neutron damage than the narrow-base (high-gain) transistors, as is expected. For those cases, where the gain of the 100% Boron-11 transistors appeared to have slightly increased in gain as a result of neutron irradiation, the $\Delta(1/\beta)$ was set equal to zero.

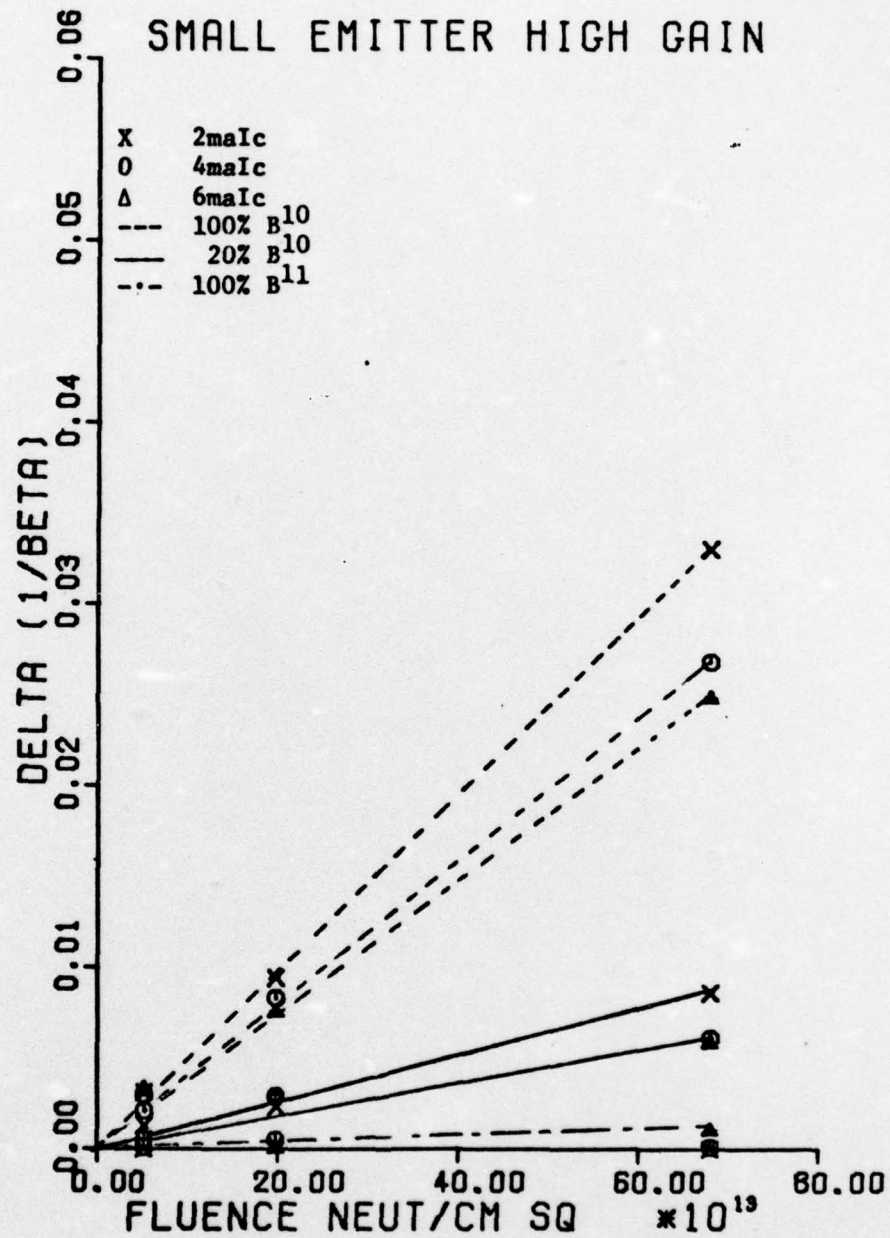


Figure 12

$\Delta(1/\beta)$ vs Fluence and Doping for Small-Emitter High-Gain Transistors

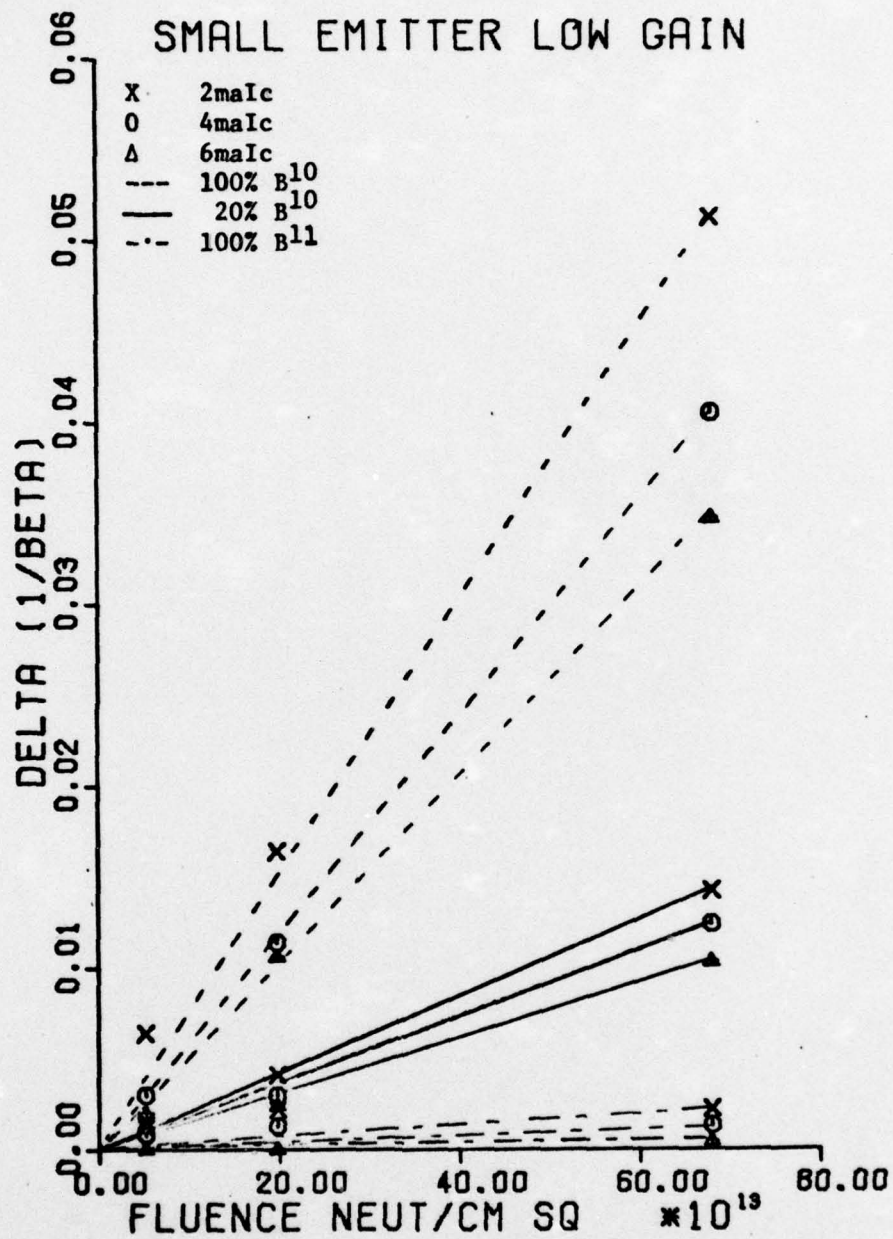


Figure 13

$\Delta(1/\beta)$ vs Fluence and Doping for Small-Emitter, Low-Gain Transistors

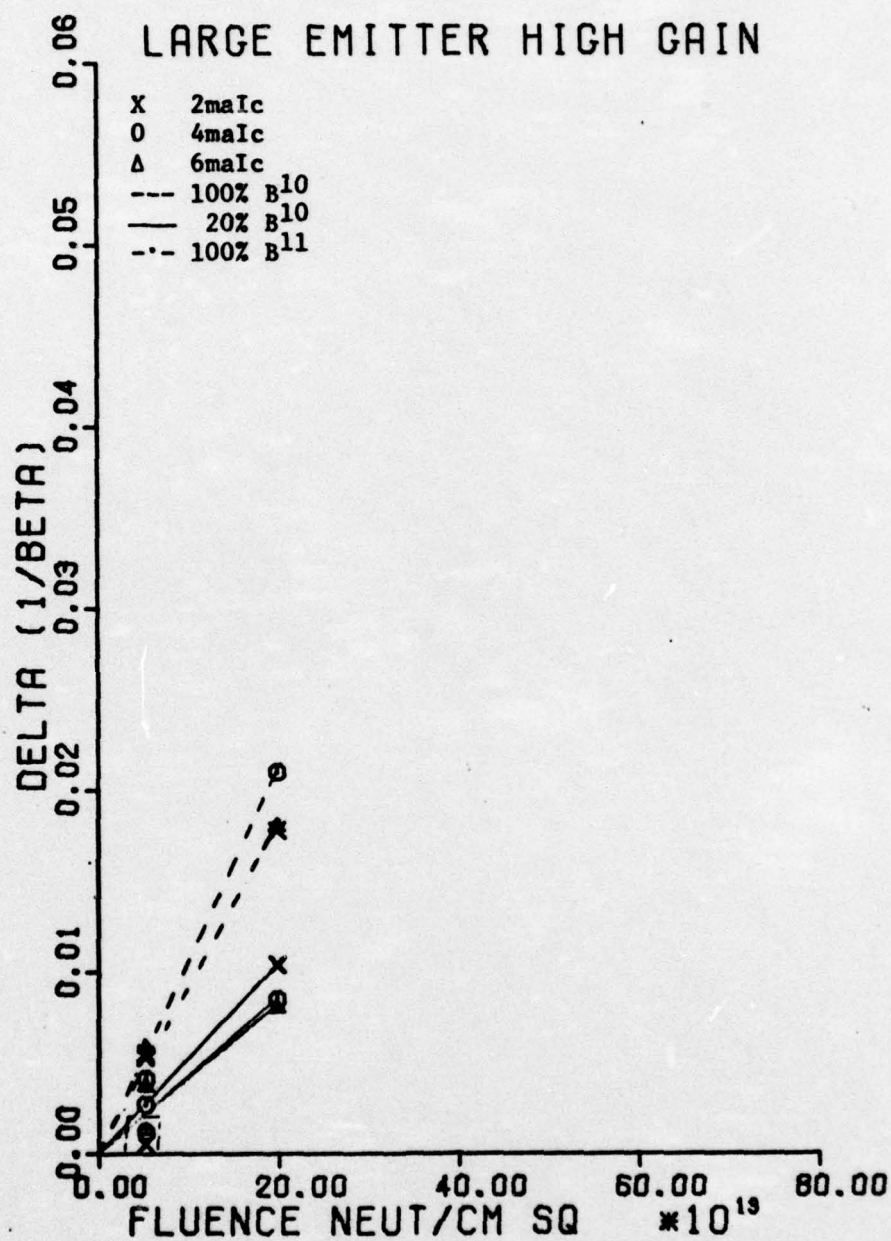


Figure 14

$\Delta(1/\beta)$ vs Fluence and Doping for Large Emitter-High Gain Transistors

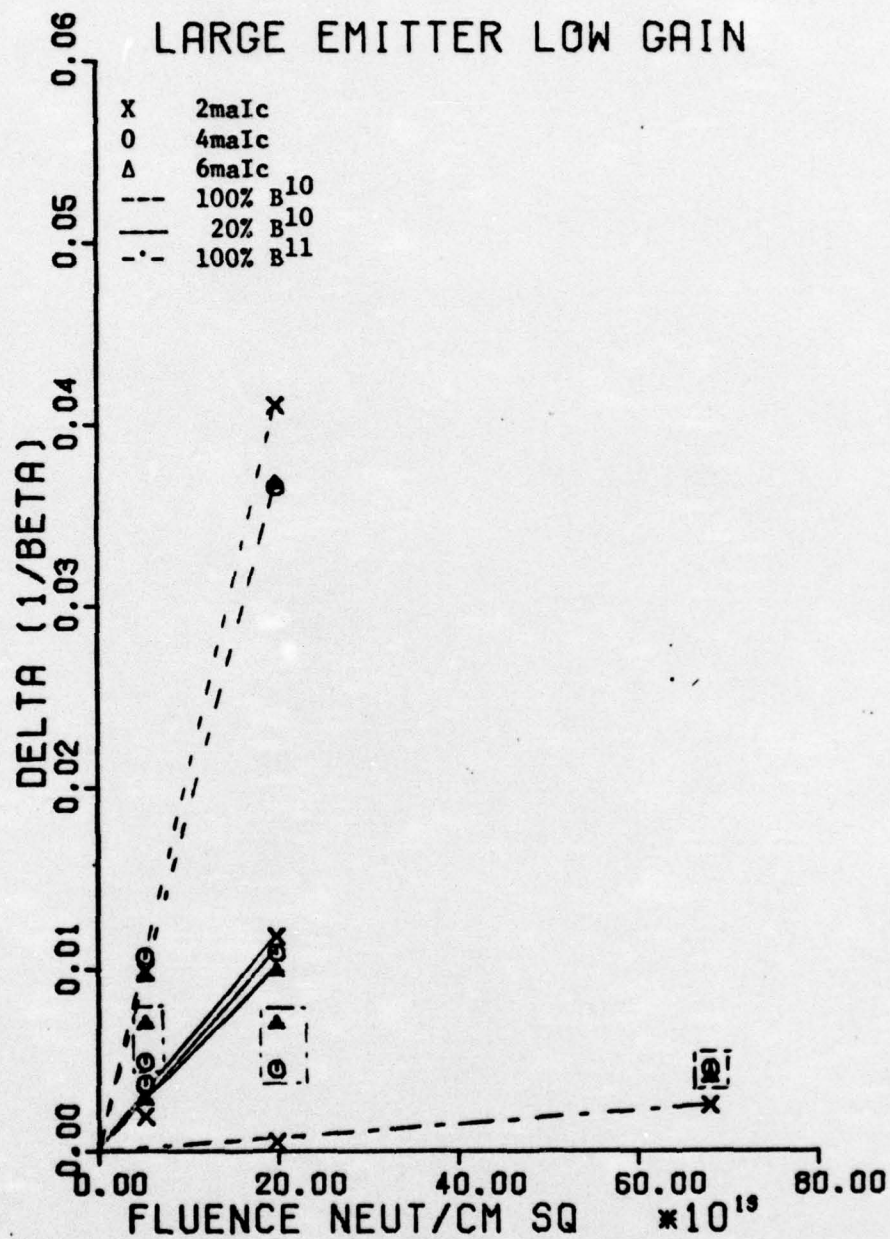


Figure 15

$\Delta(1/\beta)$ vs Fluence and Doping for Large-Emitter, Low-Gain Transistors

Since the proportionality constant between $\Delta(1/\beta)$ and neutron fluence is the radiation damage constant (C), the slopes of the curves are a measurement of C. The greater the damage the smaller the percent error due to uncertainties in the measurements. Since the uncertainties in the relative values of the flux and in the gain measurements are on the order of five percent those points near the horizontal axis are less reliable than those where the gain degradation is greater than 10%.

The second set of irradiations, which were performed by operations personnel of the National Bureau of Standards Reactor, were used to calculate the radiation damage constants for the various combinations of emitter-dopant material and device geometry used. They were also compared with bulk damage constants for the fast neutron irradiations performed by Dr. Vail to obtain the relative effectiveness of fast and thermal neutrons in producing gain degradation in these devices. A summary of these results is given in Table 1. Note the close agreement of the values of $C_{20\%B10}/C_{B10}$ to the expected value of 0.20.

Table 1

Relative Values of the Damage Constants

Relative Value - standard deviation
(number of devices used, measurements per device)

	C_{B11}/C_{B10}	$C_{20\%B10}/C_{B10}$	C_{fast}/C_{B10}
small emitter high gain	.0233±.0044 (5,5)	.190±.035 (12,4)	18.2±1.42 (12,4)
small emitter low gain	.0306±.0017 (2,3)	.243±.003 (2,3)	22.6±4.07 (4,1)
large emitter high gain	.0198±.0007 (2,3)	.197±.015 (2,3)	22.8±3.88 (4,1)
large emitter low gain	.0142±.0025 (2,3)	.143±.004 (2,3)	22.9±4.8 (4,1)

Since the high and low gain devices have the same base-dopant density and the same geometry, except for the differences in the width of the base regions, their relative values of initial gain and their relative damage constants should be in the same ratio as the square of the base widths. This follows from the fact that the time a minority carrier takes to travel across the base is proportional to the base width squared, and that the probability of recombination of a minority carrier is proportional to the time available for recombination. The ratio of the squares of the base widths, based on the control wafer measurements made by Richard Anderson, is 1.65. The various ratios of initial gains and damage constants for the high and low gain transistors is summarized in Table 2. The agreement is very good for the first two cases where there were many devices with many measurements per device.

Table 2

Comparison of High and Low Gain Devices
by initial gains and by damage constants
(number of devices used, Measurements per device)

	$\frac{\text{int. gain HG}}{\text{int. gain LG}}$	$\frac{C_{\text{fast HG}}}{C_{\text{fast LG}}}$	$\frac{C_{\text{B10 HG}}}{C_{\text{B10 LG}}}$	$\frac{C_{\text{20ZB10 HG}}}{C_{\text{20ZB10 LG}}}$
small emitter	1.65±.153 (18,11)	1.43±.26 (18,4)	1.80±.025 (6,3)	2.10±.011 (6,3)
large emitter	1.51±.182 (17,5)	1.59±.33 (17,3)	1.62±.10 (6,3)	2.27±.388 (6,3)

In Figure 16 the current dependence of the various damage constants of the small emitter high gain transistor is shown. The damage constants were normalized to those of the 100% Boron 10 by multiplying each datum point by the quotient of the average Boron 10 damage constant and the average of the damage constants to be normalized. The normalization factors used are given in the figure. This figure demonstrates that the current dependence of the damage produced by the thermal neutrons is

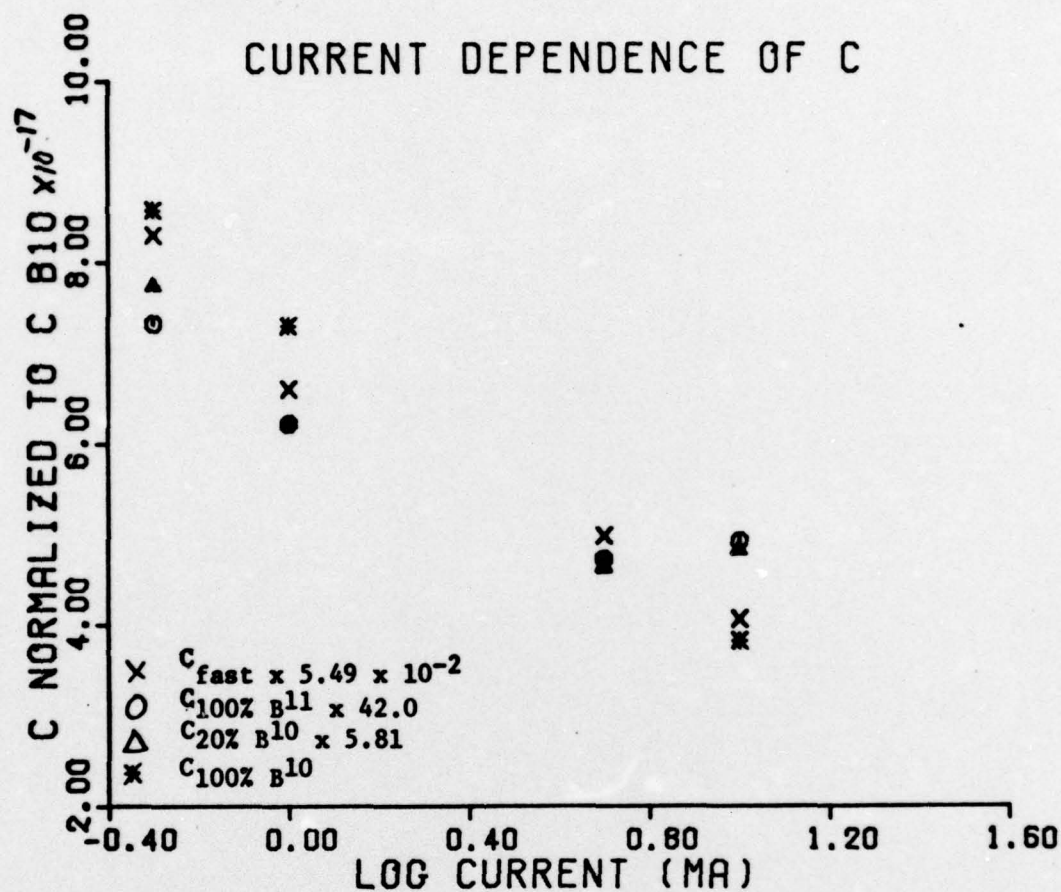


Figure 16

Current Dependence of Various Damage Constants for Small-Emitter, High-Gain Transistors

similar to that produced by fast neutrons. Insufficient comparable data points existed to make this comparison for the other transistor geometries.

The emitter and base resistances, as well as the emitter-base junction capacitances as a function of voltage and breakdown voltage of the emitter-base junction, showed no significant change as a result of the irradiations. In all but one of the 100% Boron 10, small-emitter, high-gain devices the emitter-base junction leakage changed less than 50%. However, in the devices mentioned the leakage went from 40 picoamperes to 4.2×10^6 picoamperes. As a result of this catastrophic leakage failure, the gain of this device went nearly to zero. In one of the 100% Boron-11 large-emitter devices the collector and emitter contacts appeared to have become shorted together. Two additional devices appeared to have developed open circuits in one or more contacts. The source of these catastrophic failures is unknown and these devices were not used as a data source.

The temperature monitors in the rabbit tubes indicated that the temperatures of the transistors stayed below 130°F during irradiation so that annealing effects should have been minimized. For the first set of irradiations the post irradiation gains were measured within six hours of the irradiation, and for the second set one week elapsed between the irradiation and the gain measurement. A recheck of one 100% Boron 10 device indicated that after ten days had elapsed $(12 \pm 3)\%$ of the initial damage had been annealed. For this reason the devices in each irradiation set were compared only to other devices in the same set.

When the calculations of Appendix C are applied to the fluence, doping level, and device geometry, it is found that 1.3×10^6 thermal neutron captures by Boron-10 atoms in the emitter region, produce a 50% gain degradation in the small-emitter, high-gain, 100% Boron-10 devices. Applying the

geometry factors calculated using the method given in Appendix B, gives the result that 5.6×10^4 alpha particles and 1.1×10^5 lithium nuclei do damage in the base region. In contrast, 5.1×10^4 fast neutron interactions in the base produce similar results (Ref 6). A one MeV neutron will produce 5.0×10^3 defects in silicon (Ref 4:441-445). Since the volume of the base region is only $6.4 \times 10^{-9} \text{ cm}^3$, the number of fast neutron defects would be 4.0×10^{16} per cubic centimeter. As this defect density is on the order of the base dopant density observable degradation is expected. Since the number of alpha particles and lithium atoms doing damage in the base is approximately 3.3 times greater than the fast neutrons, the lithium atoms and the alpha particles would only need to produce 2,000 defects per particle to cause the same damage. As was shown in Chapter II, 11,000 defects per alpha particle or lithium nucleus is possible.

The following equation for calculating the relative effectiveness of thermal neutrons to fast neutrons in producing defects in bipolar transistors can be obtained from these results.

$$\frac{C_{\text{thermal}}}{C_{1 \text{ MeV}}} = \frac{0.3 (G_{\alpha} + G_{Li}) \sigma_{\text{thermalB10}} N_{B10} W_{\text{Emitter}}}{\sigma_{1 \text{ MeV si}} N_{\text{si}} W_{\text{Base}}}$$

where G_{α} and G_{Li} are the geometry factors derived in Appendix B, $\sigma_{\text{thermalB10}}$ is the Thermal Group capture cross section for Boron-10, $\sigma_{1 \text{ MeV si}}$ is the one MeV scatter cross section for silicon, N_{B10} is the atom density of Boron-10 atoms in the emitter, N_{si} is the atom density of silicon in the base, W_{Emitter} is the width of the Emitter, and W_{Base} is the width of the base. This formula, which is derived in Appendix H, is good only for devices where the combined width of the emitter and base regions is less than the path length of a 0.88 MeV lithium nucleus in silicon (about $3.0 \mu\text{m}$).

At the fluence at which the 100% Boron-11 devices begin to show damage (5×10^{15} neutrons per square centimeter) the density of thermal neutron captures by silicon atoms would be 2.3×10^{13} captures per square centimeter. Since a thermal neutron capture imparts an average of 780 eV of energy to a silicon atom, the defects produced by recoil of the lattice atoms resulting from these captures was possibly the main source of degradation of the all Boron 11 devices. Also thermal neutron captures by the Boron 10 in the collector dopant may have made a significant contribution to the observable damage. Bulk displacement from Compton scatter of gamma rays probably also contributed to the damage observed in the 100% Boron-11 transistors.

CHAPTER V

CONCLUSIONS AND RECOMMENDATIONS

For each of the forty two transistors exposed to thermal neutron irradiation, the damage observed was proportional to the fraction of the emitter dopant atoms that were Boron-10. It is therefore concluded that the hypothesized source of thermal neutron damage (Ref 1) in bipolar PNP transistors is indeed the main source of the thermal neutron damage observed in this experiment. Also the thermal neutron fluence and current dependence of the gain degradation indicated that bulk displacement damage was the source of damage. It was also observed that for these transistors, where the combined width of the emitter and base regions is less than the path length of a 0.88 MeV lithium nucleus in silicon, the dependence of gain degradation on the width of the base region was roughly the same for fast and thermal neutrons. One-MeV neutrons were found to be approximately twenty times more effective than thermal neutrons in degrading the gain of the transistors with 100% Boron-10 emitter dopant atoms and one hundred times more effective in degrading the transistor doped with 20% Boron-10 and 80% Boron-11. By applying a geometry factor that was developed, it was found that a one MeV neutron produces about 3.3 times as many defects in silicon as are produced by the average particle (lithium or alpha doing damage in the base). An equation was developed to permit the calculation of the relative sensitivity of a given transistor to thermal neutron damage.

Since much of the material in the environment can conceivably thermalize neutrons from nuclear weapons, and since the effectiveness of thermal neutrons in producing damage can be reduced by using 100% Boron 11 as the dopant material, it would be desirable to use 100% Boron 11 doped

transistors in underground or underwater electronic systems that must function in a nuclear environment. However, since pure Boron-11 would be expensive, it may be more cost effective to use the relative damage equation developed to obtain device geometries more resistant to thermal neutron damage. It is therefore recommended that additional studies be made of the effectiveness of various geometries in minimizing thermal neutron damage in bipolar transistors, and that this information be used to test and improve the analytical method developed to predict thermal neutron damage in bipolar transistors.

BIBLIOGRAPHY

1. Arimura, I. and C. Rosenberg. "Anomalous Damage Mechanism in PNP Silicon Transistors Due to Thermal Neutrons." IEEE Transactions on Nuclear Science, NS-20 6:274-279 (December 1973).
2. Becker, D. A. "Flux Information on Thermal Column Pneumatic Tube Facility". Unpublished data sheet. Available from the National Bureau of Standards, Reactor Operations Division, Gaithersburg, Maryland.
3. Brophy, James J. Basic Electronics for Scientists. New York: McGraw Hill Inc., 1969.
4. Buehler, Martin G. Microelectronic Test Patterns: An Overview. NBS Special Publication 400-6. National Bureau of Standards, Washington D. C. August 1974.
5. Cleland, J. W. "Transmutation Doping and Recoil Effects in Semiconductors Exposed to Thermal Neutrons." Proceedings of the International School of Physics Enrico Fermi, Radiation Damage in Solids. New York: Academic Press 1962.
6. Crawford, J. H. "Radiation Effects in Ionic Crystals" in The Interaction of Radiation with Solids, Edited by R. Stumae. Amsterdam: North Holland Publishing Co. 1964.
7. Davies, John A., and L. Erikson, and J. W. Mayer. Ion Implantation in Semiconductors. New York: Academic Press 1970.
8. Donovan, R. P., and J. R. Hauser, and M. Simon. "A Survey of the Vulnerability of Contemporary Semiconductor Components to Nuclear Radiation." AFAL-TR-74-61 Air Force Avionics Laboratory, Wright-Patterson AFB, Ohio.
9. Hughes, Donald J. and Robert B. Schwart. Neutron Cross Sections, BNL 325, Brookhaven National Laboratory Associated Universities, 1 July 1958.
10. Larin, Frank. Radiation Effects in Semiconductor Devices. New York: John Wiley and Sons, Inc., 1968.
11. Leibfried, G. "Introduction into Radiation Damage Theory" in The Interaction of Radiation with Solids, Edited by R. Stumae. Amsterdam: North Holland Publishing Co. 1964.
12. McKelvey, John P. Solid State and Semiconductor Physics. New York: Harper and Row. 1966.
13. Messenger, George C. "A General Proof of the Degradation Equation for Bulk Displacement Damage". IEEE Transactions on Nuclear Science, NS-20, 1:809-810 (February 1973).

BIBLIOGRAPHY (con't)

14. "NBS Reactor," Public Information Sheet on the National Bureau of Standards Reactor, Gaithersburg, Maryland, (FJS 1969).
15. Price, William J. Nuclear Radiation Detection, New York: McGraw-Hill, Inc., 1964.
16. Raby, T. Private communication on the characteristics of the NBS Reactor Thermal Column. 22 June 1976.
17. Ramsey, C. and Patrick Vail. "Current Dependence of the Neutron Damage Factor", IEEE Transactions on Nuclear Science, NS-17, 6:310-335.
18. Ricketts, L. W. Fundamentals of Nuclear Hardening of Electronic Equipment. New York: Wiley-Interscience, Inc., 1972.
19. Vail, Patrick. Unpublished paper on calculation of reaction rate of neutrons absorbed in boron doped transistors. Air Force Weapons Lab, Kirtland AFB, New Mexico (received April 1976).

APPENDIX A

**A General Proof of the δ Degradation Equation
for Bulk Displacement Damage by George C. Messenger**

**Copyright 1973 by the Institute of Electrical and Electronic Engineers,
Inc. Reprinted, with permission, from IEEE TRANSACTIONS on Nuclear
Science, February 1973, Vol. NS-20, No. 1.**

A GENERAL PROOF OF THE β DEGRADATION EQUATION FOR BULK DISPLACEMENT DAMAGE

by George C. Messenger

ABSTRACT

A general proof for the β degradation equation in displacement producing radiation environments is presented. The proof is straightforward for the base component of damage. An extension of the proof encompasses damage in the base emitter field region to the extent it can be related to the emitter time constant. The derivation assumes a significant post-radiation common emitter current gain ($\beta > 3$).

The relationship between common-emitter current gain and displacement damage has been given as (1)

$$\frac{1}{\beta} = \frac{1}{\beta_1} + \frac{\phi}{\omega_T K} \quad (1)$$

where β is common-emitter current gain, β_1 is the initial unirradiated value of common-emitter current gain, ω_T is 2π times the common emitter gain bandwidth product, ϕ is the damaging radiation fluence and K is the relevant lifetime damage constant. This relationship was initially proven for homogeneous base transistors and later extended to cover exponentially graded base transistors (2). The following proof will show that this relationship is true for any base doping profile as long as the transistor retains a significant common-emitter current gain ($\beta > 3$).

Gover (3) has shown that for any arbitrary base impurity distribution, the series expansion for the base transport factor is

$$a = 1 - U_1 \frac{W^2}{L^2} + U_2 \frac{W^4}{L^4} - \dots \quad (2)$$

where a is the base transport factor, W is the base width and $L = \sqrt{D\tau}$ is the diffusion length. The coefficients U_1, U_2 , etc., are determined by successive iteration of the equation pair.

$$a(X) = -\frac{1}{qN} \int_X^{X_2} \frac{N}{D} J dX \quad (3)$$

$$J(X) = J^0 + q \int_{X_1}^{X_2} \frac{p}{\tau} dX$$

where a is the excess minority carrier concentration in the base, N is the impurity density in the base, D is diffusion constant, τ is minority carrier lifetime, q is electron charge, and J is minority current density.

Specifically, this procedure leads to the following deterministic equations for U_1 and U_2 :

$$U_1 = \frac{D(X_2) - (X_2)}{W^2} \int_{X_1}^{X_2} \frac{dX}{\tau(X) N(X)} \int_X^{X_2} \frac{N(\bar{X}) d\bar{X}}{D(\bar{X})} \quad (4)$$

$$U_2 = \frac{D^2(X_2) - (X_2)^2}{W^4} \int_{X_1}^{X_2} \frac{dX}{\tau(X) N(X)} \int_X^{X_2} \frac{N(\bar{X}) d\bar{X}}{D(\bar{X})}$$

$$\int_{X_1}^X \frac{d\bar{X}}{\tau(\bar{X}) N(\bar{X})} \int_{\bar{X}}^{X_2} \frac{N(\bar{X}) d\bar{X}}{D(\bar{X})}$$

A recombination series corresponding to Equation (2) exists for n and j .

$$J(X) = J^0(X) + J^1(X) + \dots$$

$$n(X) = n^0(X) + n^1(X) + \dots \quad (5)$$

Now,

$$1 - a = \frac{-J^1 + J^2 + J^3 \dots}{J^0} = -\frac{J^1}{J^0} \quad (6)$$

The series expansion is rapidly convergent and can be terminated at J^1 since

$$U_2 \frac{W^4}{L^4} < U_1 \frac{W^2}{L^2} \text{ except for transistors so seriously}$$

damaged that they are no longer of practical interest.

From Equation (2) and assuming that base transport is the dominant factor in the radiation dependence of common emitter current gain

$$\frac{1}{\beta} = \frac{U_1 W^2}{D \tau} \quad (7)$$

Gover (3) also shows that when n/τ is described by a single time constant, i.e.,

$$\frac{1}{q} \frac{\partial J}{\partial X} = \frac{p}{\tau} (1 + j\omega\tau), \quad \omega_T = \frac{D}{U_1 W^2} \quad (8)$$

again truncating the recombination series at the first-order term.

Now minority carrier lifetime as a function of displacement fluence is given by

$$\frac{1}{\tau} = \frac{1}{\tau_1} + \frac{\phi}{K} \quad (9)$$

For all damaging radiations including neutrons, protons, electrons and γ rays with the appropriate choice of K .

Combining this result with Equation (7) gives

$$\frac{1}{\beta} = \frac{1}{\beta_1} + \frac{U_1 w^2}{D} + \frac{\phi}{K} \quad (10)$$

Note that $\frac{1}{\beta_1}$ may also contain a surface recombination, and an emitter efficiency contribution as long as they do not change significantly with displacement fluence.

Combining this result with Equation (8) gives

$$\frac{1}{\beta} = \frac{1}{\beta_1} + \frac{\phi}{\tau K} \quad \text{Q. E. D.} \quad (11)$$

The base impurity distribution is arbitrary, both τ and D may be functions of X , but the transistor must have significant common-emitter current gain, i.e.,

$$U_2 \frac{w^4}{L^4} \ll U_1 \frac{w^2}{L^2}$$

Values of U_1 and U_2 are given in Table 1 for homogeneous and exponential impurity distributions. The error function impurity distribution produces U_1 and U_2 values very similar to the exponential distribution.

Homogeneous Base		Exponential Base
$N = \text{Const.}$		$N = N_0 e^{-\eta x/w}$
U_1	$\frac{1}{2}$	$\frac{\eta + e^{-\eta} - 1}{\eta^2}$
U_2	$\frac{5}{24}$	$\frac{\frac{1}{2}\eta^2 - 2 + (3\eta + 1)e^{-\eta} + e^{-2\eta}}{\eta^4}$

Table 1

Values of U_1 and U_2 for Homogeneous and Exponential Impurity Distribution with D and τ constant.

Ramsey and Vail⁽⁴⁾ have shown that the emitter efficiency contribution resulting from recombination in the emitter base field region can be related to the emitter time

constant, $\tau_e C_e$. Equation (9) strictly relates to the cut-off frequency for base transport; it can be readily extended to include the emitter time constant.

$$\omega_T = (r_e C_e + \frac{U_1 w^2}{D})^{-1} \quad (12)$$

Including both emitter-base field recombination and base recombination and extending Equation (7) including the Ramsey and Vail⁽⁴⁾ relationships.

$$\frac{1}{\beta} = \frac{U_1 w^2}{D\tau} + \frac{1}{\tau K} = \frac{1}{\tau} (r_e C_e + \frac{U_1 w^2}{D}) \quad (13)$$

Combining Equations (12), (13) and (9) yields

$$\frac{1}{\beta} = \frac{1}{\beta_1} + \frac{\phi}{\tau K} \quad \text{Q. E. D.} \quad (14)$$

This extends the proof to cover both emitter-base field recombination and bulk recombination subject to the additional approximations used by Ramsey and Vail⁽⁴⁾ to obtain Equation (13).

References

- (1) Messenger, G. C. and Spratt, J. P. "The Effects of Neutron Irradiation on Germanium and Silicon," New York Meeting of Electrochemical Society, April 1958. Published in Proceedings IRE, June 1958, pp 1038-1044.
- (2) Messenger, G. C. "Current Gain Degradation due to Displacement Damage for Graded Base Transistors," Proc. IEEE Vol. 55 No. 3, March 1967, pp 160.
- (3) Gover, et al "Bipolar Transistor Base Parameters and Impurities," PGED-19 Vol. 8, August 1972, pp 967-975.
- (4) C. Ramsey and P. Vail "Current Dependence of the Neutron Damage Factor," PGNS Vol. NS-17 No. 6, pp 310-135.

COPY AVAILABLE TO DDC DOES NOT
PERMIT FULLY LEGIBLE PRODUCTION

APPENDIX B
GEOMETRY FACTOR CALCULATION

The geometry factor is the portion of particles produced in the emitter that do all of their damage in the base region. This calculation of the geometry factor requires the following assumptions:

- 1) All directions of particle emission are equally probable;
- 2) The path length of the particles is short compared to the surface area of the devices;
- 3) That the range of the particle is greater than the thickness of the emitter and base regions; and
- 4) That the particle does all of its displacement damage at the end of its path length.

Then the locus of points at which a particle originating at a given location can do damage would form a sphere of radius equal to the range of the particle, with its center at the point of origin. By assumption 3 the sphere must contain a complete thickness of the slab of the base region (see Figure B1).

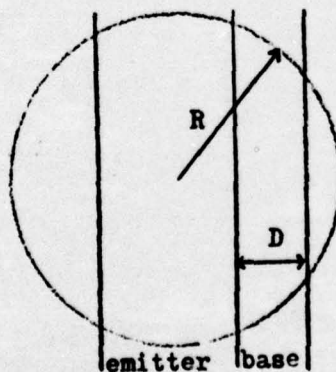


Figure B1
Geometry Factor Relationships

Let the range of the particle be R and the thickness of the base region be D . Then the area S of the intersection of the sphere with the base region is just

$$S = 2 \pi R D$$

This is true regardless of the position of the slab in the sphere as long as a complete base region width is contained in the sphere as required by assumption 3. The total area of the sphere A is:

$$A = 4 \pi R^2$$

Since A is a measure of all possible damage sites and S is a measure of those in the base region the fraction produced that ends in the base region is just S/A or

$$G = \frac{D}{2R}$$

where G is the fraction of total particles produced that do damage in the base region. Note that the distribution of sources across the emitter region is unimportant as long as assumptions 1 through 4 are met.

APPENDIX C

THERMAL NEUTRON REACTION RATE IN PNP TRANSISTORS by Patrick J. Vail (Ref. 19)

The B^{10} (n, α) Li^7 reaction is exothermic with an energy release of 2.78 MeV. In reactions involving thermal neutrons the probability of forming Li^7 in the ground state is only 0.064. Instead, an intermediate excited state of Li^7 is formed, followed by the emission of a 0.48 MeV Gamma ray. Thus the total kinetic energy available to the Li^7 nucleus and the alpha as follows:

$$E_{Li} = \frac{E_{KE} M_{\alpha}}{M_{\alpha} + M_{Li}} = \frac{(2.30)(4.00)}{(4.00) + (7.02)} = 0.83 \text{ MeV} \quad (1)$$

$$E_{\alpha} = \frac{E_{KE} M_{Li}}{M_{Li} + M_{\alpha}} = 1.47 \text{ MeV} \quad (2)$$

Up to 30 keV the cross section, σ , for this reaction has a $1/v$ dependence, where v is the thermal neutron velocity. This can be represented as follows:

$$\sigma = \frac{\sigma_0 v_0}{v} \quad (3)$$

where $v_0 = 2.2 \times 10^5$ cm/sec and $\sigma_0 = 3840$ barns = 3.84×10^{-21} cm².

This $1/v$ dependence can be used to calculate the reaction rate, dR , resulting from neutrons with energies between E and $E + dE$ in the volume element dV :

$$dR = N(x,y,z) \sigma(E) \phi(E,x,y,z) dE dV \quad (4)$$

where $N(x,y,z)$ = the number of B^{10} atoms per unit volume at the point (x,y,z) , $\sigma(E)$ = the B^{10} (n, α) cross section at energy E corresponding to the velocity V through the equation $E = \frac{1}{2} m_n v^2$, and $\phi(E,x,y,z) =$

the flux per unit energy interval at the point (x,y,z). Since the flux is for our purposes assumed to be independent of position we may write:

$$\phi(E,x,y,z) = \phi(E) \quad (5)$$

We can also write:

$$\phi(E) = n(E)v \quad (6)$$

where $n(E)$ is the number of thermal neutrons per unit volume per unit energy interval with energies between E and $E+dE$. Combining equations (3) and (6), we get:

$$\begin{aligned} \phi(E) \sigma(E) &= [n(E)v] [\sigma_0 v_0 / v] = \\ &= n(E) \sigma_0 v_0 \end{aligned} \quad (7)$$

The resulting expression for dR is thus:

$$dR = N(x,y,z) n(E) \sigma_0 v_0 dE dV \quad (8)$$

This may be integrated to yield the total number of reactions, R , produced by an arbitrary spectrum of neutrons with energies below 30 KeV:

$$\begin{aligned} R &= \sigma_0 v_0 \int_{Vol} \int_0^{30 \text{ KeV}} N(x,y,z) n(E) dE dV = \\ &= \sigma_0 v_0 \int_{Vol} N(x,y,z) dV \int_0^{30 \text{ KeV}} n(E) dE \end{aligned} \quad (9)$$

Here:

$$\int_{Vol} N(x,y,z) dV = N_B \quad (10)$$

where N_B = total number of Boron¹⁰ atoms in sample, and

$$\int_0^{30 \text{ KeV}} n(E) dE = n \quad (11)$$

where n is the number of neutrons per unit volume, irrespective of energy up to 30 keV incident on the sample.

Thus:

$$R = N_B \sigma_0 v_0 n \quad (12)$$

Note that equation (12) is independent of both the neutron spectrum and of the distribution of the boron atoms in the sample. Equation (12) can be expressed in terms of the neutron flux, $\phi = n \bar{v}$, where \bar{v} is the average neutron velocity:

$$R = \frac{N_B \sigma_0 v_0}{\bar{v}} \phi \quad (13)$$

For a Maxwell-Boltzman distribution in thermal neutron energy, \bar{v} is 1.128 v_0 at 20°C. For this spectrum:

$$R = \frac{N_B \sigma_0 \phi}{1.128} \quad (14)$$

The above equation can also be expressed in terms of the total neutron fluence, Φ , incident on the sample in time t . Here we will assume that the neutrons are deposited uniformly in time and write:

$$\Phi = \phi t \quad (15)$$

Thus we may write:

$$R = \frac{N_B \sigma_0 \Phi}{(1.128)t} \quad (16)$$

The total number, N , of alphas produced is:

$$N_\alpha = Rt = \frac{N_B \sigma_0 \Phi}{(1.128)} \quad (17)$$

or since $\sigma_0 = 3.84 \times 10^{-21} \text{ cm}^2$:

$$N_\alpha = (3.4 \times 10^{-21} \text{ cm}^2) N_B \Phi \quad (18)$$

Note that only 18.45 to 18.98% of naturally occurring boron is B¹⁰. The bulk of naturally occurring boron is B¹¹.

Let us now consider a specific example of a PNP bipolar transistor whose emitter is heavily doped with boron. Typical dopant concentrations

at the junction between the emitter and the base are 10^{20} boron atoms per cm^3 . Let us also assume that this transistor is irradiated by thermal neutrons with a Maxwell-Boltzman spectrum to a fluence of $5 \times 10^{11} \text{ n/cm}^2$. Further, let us assume that the PNP transistor is of planar construction with a base width of 0.7 microns and an emitter width of 1.3 microns. Since the range of an alpha particle from the $\text{B}^{10} (\text{n}, \alpha) \text{Li}^7$ reaction is 10 microns, the alpha penetrates far into the collector where most of its energy is dissipated. Let us assume also that the emitter is 1 mil x 1.5 mils in area. Since there are 25.4 microns to a mil these dimensions are large compared to the range of the alpha. We can thus calculate the total number of boron (n, α) reactions which occur by use of equation (18).

$$N_{\alpha} = (3.4 \times 10^{-21} \text{ cm}^2) \phi N_B \quad (19)$$

$$= (1.7 \times 10^{-9}) N_B$$

$$= (1.7 \times 10^{-9}) (10^{20} \frac{\text{B}}{\text{cm}^3}) (2.5 \times 10^{-3} \text{ cm}) \times$$

$$(3.75 \times 10^{-3} \text{ cm}) (1.3 \times 10^{-4} \text{ cm}) (.1898 \text{ B}^{10}/\text{B})$$

$$N_{\alpha} = 39.3 \text{ alphas} = N_{\text{Li}} = 39.3 \text{ Li}^7 \text{ atoms}$$

Since half of these alphas are directed toward the surface we get the result that there are only 20 alpha which penetrate the base region. Since this is such a small number of alphas we may neglect any damage or ionization produced. For example, we may assume for a worst case ionization condition that all of the energy of the alpha and the lithium recoil atom goes into ionization. The result will be no more than a thousand rads silicon deposited in the transistor even when the short range of the lithium recoil is considered in a calculation of effective collection volume. Note that a rad is an expression of energy per gram

and as the collection volume decreases, the rads deposited will increase in this case. Increasing the emitter area does not have any effect on the rads deposited for this same reason. It is also easy to see that the damage due to 20 alphas and 20 Li^7 nuclei will also be negligible. Increasing the area also has no effect on the ratio of damage to area, which determines the degradation. Only an increase of doping level and emitter thickness to unrealistic dimensions will yield enough alphas to degrade the transistor.

APPENDIX D

NBS-2 TEST PATTERN

by Martin G. Buehler

Note: All dimensions in mils. Center of mask is taken as (0,0); horizontal coordinate is given first followed by vertical coordinate. One square equals one mil. Lines not on grid lines are halfway between grid lines. C=Center. R=Radius. S=Distance from C to one side of square.

Table D1
Test Structures
Numbers refer to Figure D1

Number	Test Structure	Dimension, ^a mil
1	Gated circular base-collector junction with diffused channel stop	D = 6
2	Ungated circular base-collector junction with diffused channel stop	D = 6
3	Ungated square base-collector junction with diffused channel stop	S' = 5
4	Gated square base-collector junction with diffused channel stop	S' = 18
5	Ungated circular base-collector junction with diffused channel stop	D = 20
6	Gated circular base-collector junction with diffused channel stop	D = 20
7	Gated circular base-collector junction (small emitter) with diffused channel stop	D = 20
8	Gated circular base-collector junction (large emitter) with diffused channel stop	D = 20
9	Gated circular base-collector junction with diffused channel stop	D = 60
10	MOS capacitor over collector with field plate and diffused channel stop	D = 6
11	MOS capacitor over collector with field plate and diffused channel stop	D = 20
12	MOS capacitor over collector with distant field plate and diffused channel stop	D = 20
13	MOS capacitor over base without field plate and diffused channel stop	D = 20
14	Base sheet resistor	
15	Emitter sheet resistor	
16	Metal-to-base contact resistor	
17	Metal-to-emitter contact resistor	
18	Collector resistor	
19	Base-under-the-emitter sheet resistor (tetrode transistor)	
20	Hall effect pattern	
21	Alignment marker	

^a D = diameter of a circle, S' = side of a square. Tolerances should be held to ± 0.1 mil. If metric dimensions are desired the diameters should be 0.15 mm (for structures numbered 1, 2, 10), 0.5 mm (5-8, 11-13), and 1.5 mm (9), and the sides should be 0.13 mm (3) and 0.46 mm (4); all tolerances should be held to ± 0.002 mm.

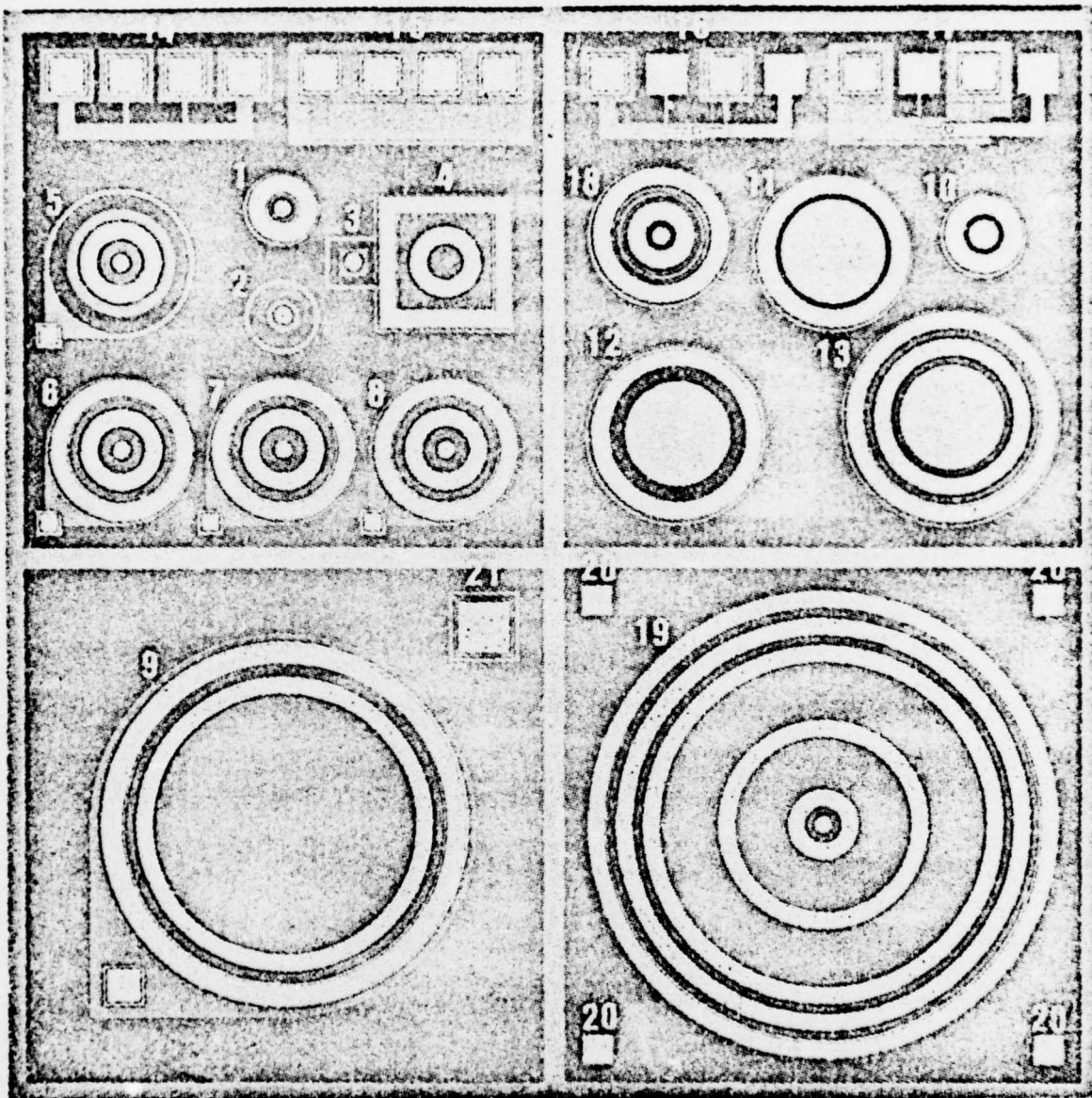


Figure D1

Test pattern, NBS-2, for characterizing the electrical properties of silicon MOS capacitors and p-n junctions. (The 21 elements are identified in table D1. The overall pattern is 200 mil (5.08 mm) on a side.)

BASE MASK

(For positive photoresist black areas are clear on final mask)

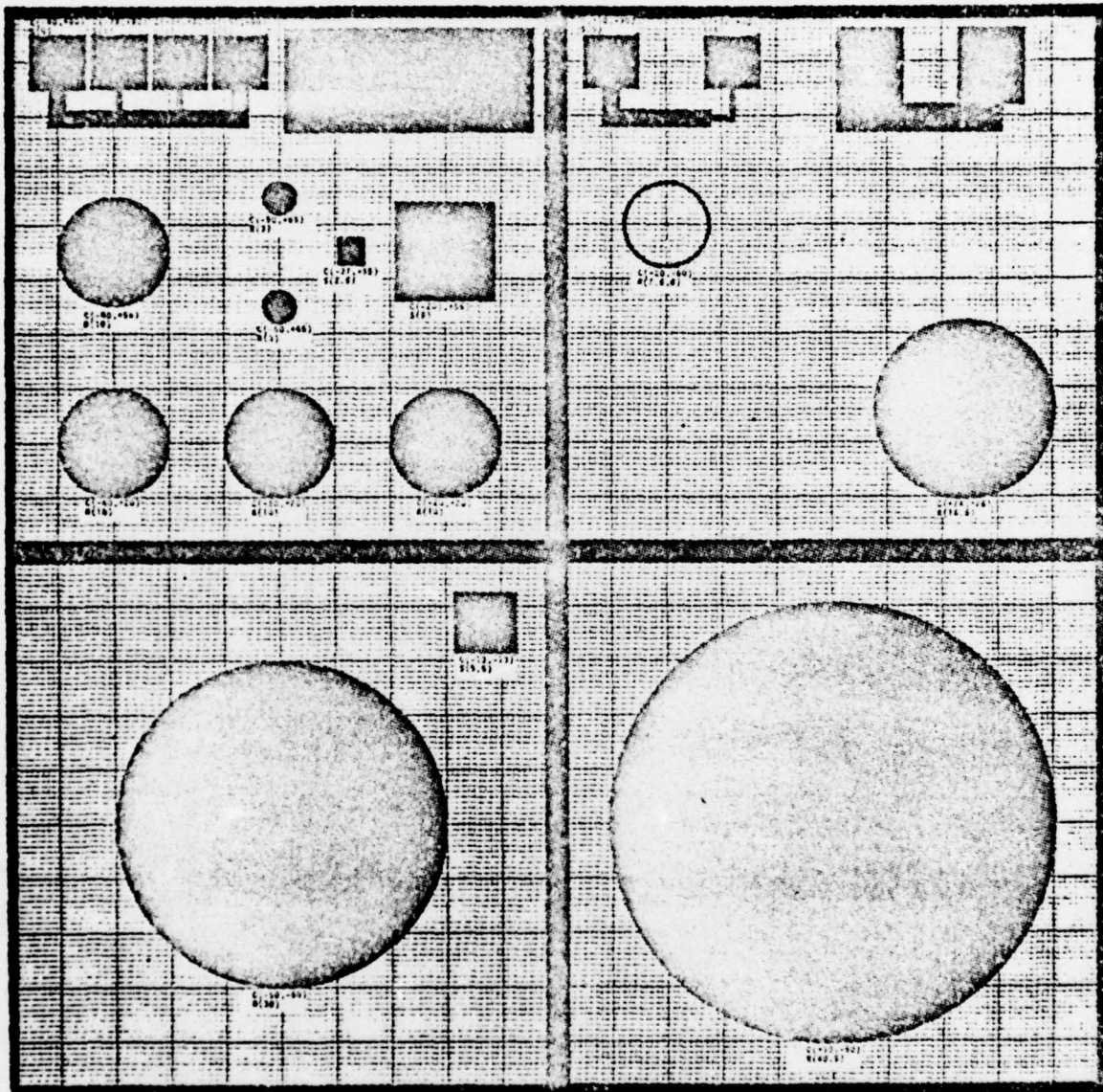


Figure D2

Base Mask

EMITTER MASK

(For positive photoresist black areas are clear on final mask)

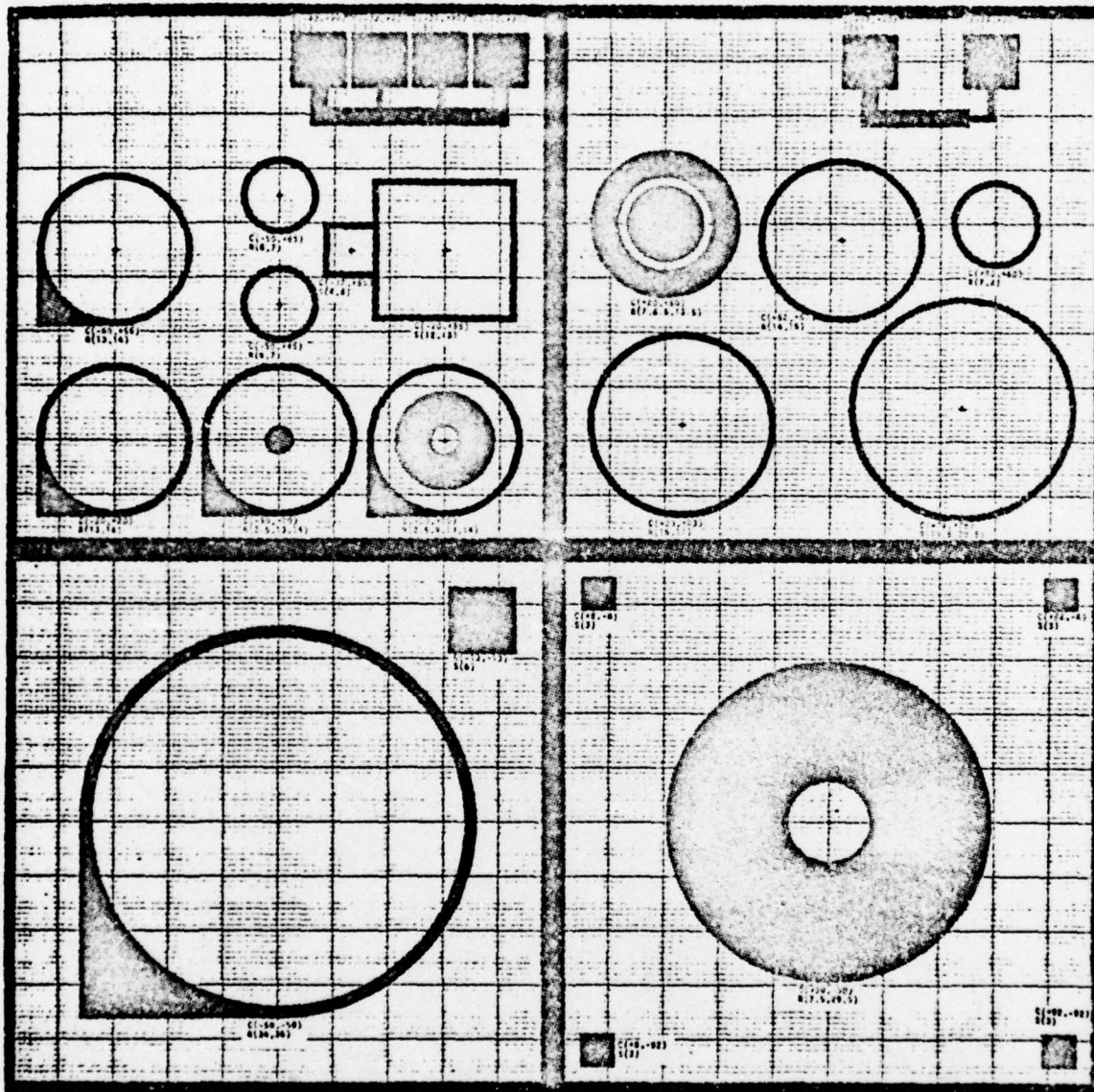
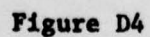


Figure D3

Emitter Mask

(For positive photoresist black areas are clear on final mask)



Contact Mask

**COPY AVAILABLE TO DDC DOES NOT
PERMIT FULLY LEGIBLE PRODUCTION**

METAL MASK

(For positive photoresist black areas are black on final mask)

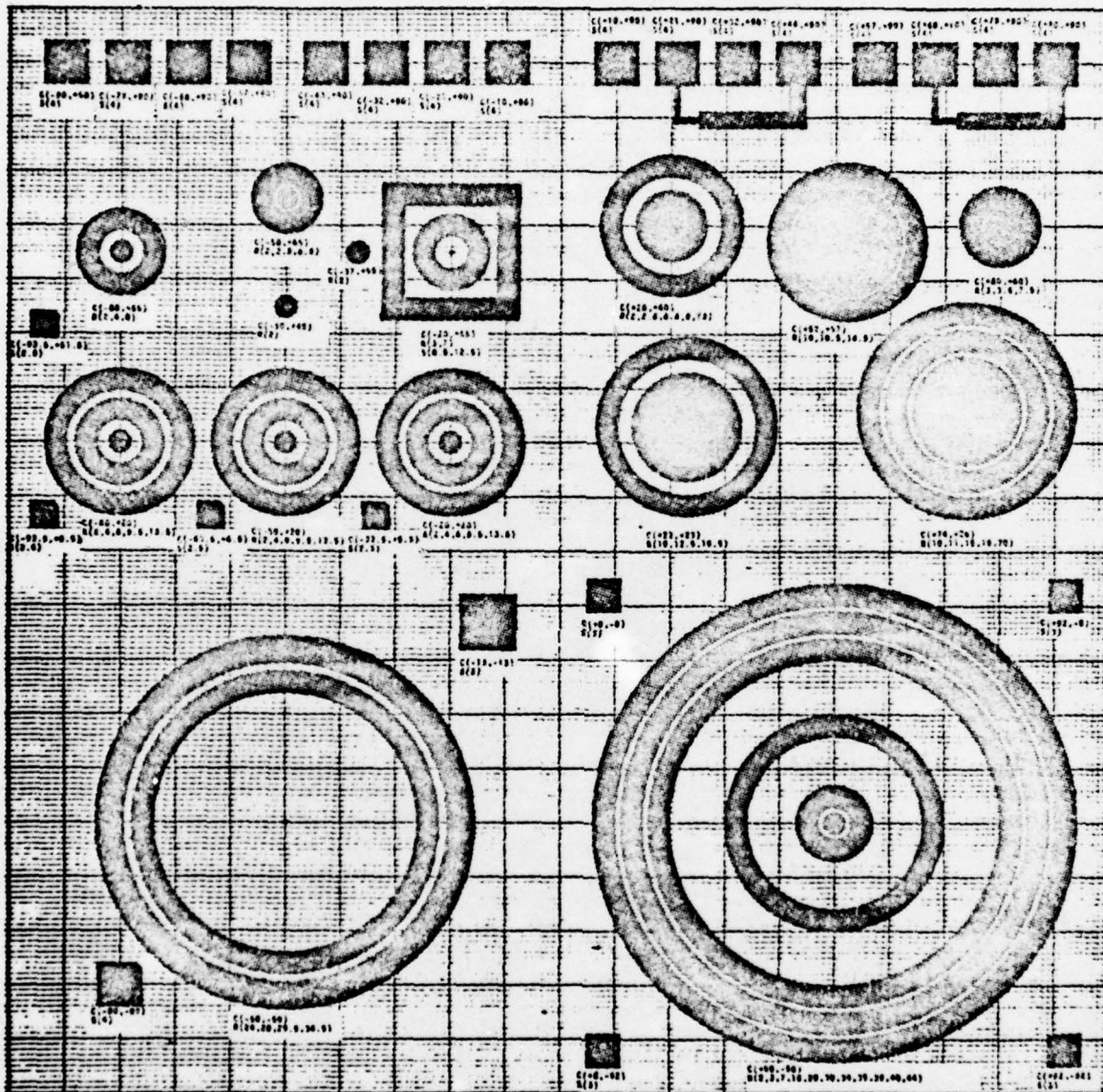


Figure D5

Metal Mask

COPY AVAILABLE TO DDC DOES NOT
PERMIT FULLY LEGIBLE PRODUCTION

APPENDIX E

Transistor Process Information

by Richard E. Anderson

Control Wafer Measurements

- C1 - Base Implant, drive-in A Drive-in B: we,4,2,8,4,12
 Rs = 193 Ω/\square Drive-in A: w1,2,5,6,9,10
 Xj = 1.55 μm
- C2 - ^{11}B Emitter + base, drive-in A
 Rs = 24.8 Ω/\square
 Xj = 1.05 μm
- C3 - ^{11}B Emitter + base, drive-in B
 Rs = 24.6 Ω/\square
 Xj = 1.09 μm
- C4 - ^{10}B Emitter + base, drive-in A
 Rs = 25.0 Ω/\square
 Xj = 0.90 μm
- C5 - 80% ^{11}B + 20% ^{10}B emitter + base, drive-in A
 Rs = 25.3 Ω/\square
 Xj = 0.93 μm

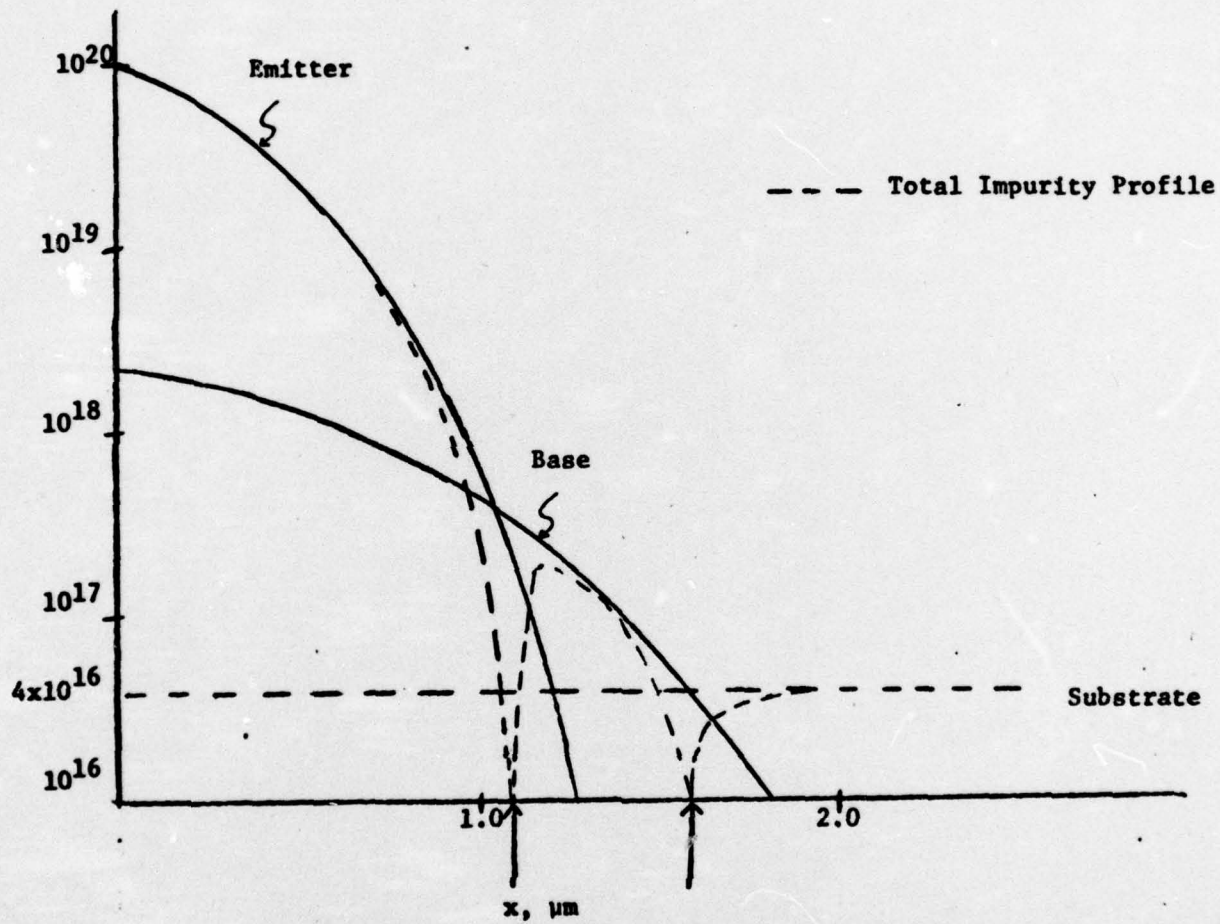
For Base: $\bar{\sigma} = \frac{1}{R_s X_j} = 33.4 (\Omega\text{-cm})^{-1}$

from Irvin's Curves $C_s \approx 2 \times 10^{18} \text{cm}^{-3}$ (for 10^{12} substrate)
 (Gaussian)

For Emitter $\bar{\sigma} = \frac{1}{R_s X_j} \approx 400 (\Omega\text{-cm})^{-1}$

from Irvin's Curves $C_s \approx 10^{20} \text{cm}^{-3}$ (for 10^{12} substrate)
 (Gaussian)

Approximate Impurity Profiles
Based on Gussion profiles using Irvin's Curves



Base
Width
 $\sim 0.5 \mu\text{m}$

Figure E1
Doping Profile

These curves are hand-down fits through C_s and X_j points, so are merely representations of actual profiles.

Packaged Device Pin Connections

Notation: Each can has a number scratched on the lid.

4A - Devices from wafer 4, chip A

[chip A contains small transistor (structure #7) and emitter resistor (structure 15)]

4B - Devices from wafer 4, chip B

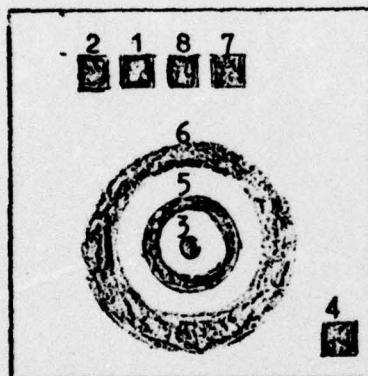
[Chip B contains structure #19, tetrode transistor]

similarly for others such as

2A, 2B, 6A, 6B, etc. In each case the number refers to the wafer number.
See process sequence.

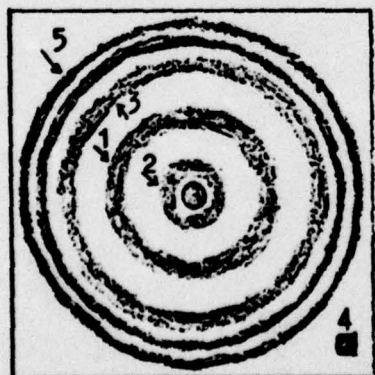
Pin Connections

Chip A



pin 6 is field plate
at collector-base junction

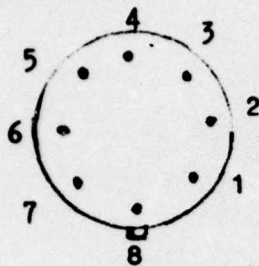
Chip B



pin 5 is field plate at
collector base junction

pins 3 & 2 are base contacts

TO-5 Headers



Top View pin numbering

- pin 4 is shorted to header -
thus is used for collector.

Each can lid has number identifying wafer and type of chip contained therein.

Wafer numbers refer to processing sequence

Wafer Nos.: 2 - ^{11}B emitter, $\beta \sim 40$
4 - ^{11}B emitter, $\beta \sim 75$
6 - ^{10}B emitter, $\beta \sim 40$
8 - ^{10}B emitter, $\beta \sim 75$
10 - $0.8^{11}B + 0.2^{10}B$, $\beta \sim 40$
12 - $0.8^{11}B + 0.2^{10}B$, $\beta \sim 75$

Note that β may vary somewhat from device to device

Chip A: Small emitter transistor and emitter resistor

Chip B: Tetrode transistor (base-under-emitter resistor)

Process Sequence for D0301A Bipolar Transistors

Wafers are P-Boron (100) 0.4-0.6 Ω -cm
NBS-2 Mask Set

12 Active
5 Controls

1. Acid Clean	A+C
2. Dry/Steam Oxide; 15/90 min, 1100°C	A+C
3. Neg. PR, lev 1 (base)	A
4. BOE Etch	A+C
5. Clean (PR strip)	A
6. Phos Implant; 1.3×10^{14} at 160 keV	A+C
7. Etch 4 min ($\sim 4000\text{\AA}$)	A+C
8. Base drive-in, Dry O_2 , 1100°C, 120 min	A+C
9. Neg. PR, lev. 2 (emitter)	A
10. Etch	A+C2-C5
11. Boron Implant; $11B+5 \times 10^{15}$ at 60 keV	W 1-4, C2, C3
12. Boron Implant; $10B+5 \times 10^{15}$ at 60 keV	W 5-8, C4
13. Boron Implant; 80% $11B+$, 20% $10B+$ 5×10^{15} , 60 keV	W9-12, C5
14. Clean (PR strip)	A
15. Deposit $5 \times \text{\AA}$ oxide	A+C
16. Emitter drive-in; 1000°C, 30 min, N_2	A+C
17. Emitter drive-in; 1000°C, 30 min, N_2	W3,4,7,8,11,12,C3
18. Neg. PR, Lev. 3 (contact)	A
19. Etch	A+C
20. Clean (PR strip)	A
21. Probe wafer-gain measurement	
22. Clean	
23. Drive-in; 1100°C, 15 min, N_2	W1, 3
24. 30 sec Etch	W1, 3
25. Probe wafer	
26. Drive-in; 1100°C, 12 min, N_2	A+C except W1, 3
27. 15 sec Etch	A+C except W1,3
28. Probe wafer	
29. Clean	A+C
30. Drive-in; 1000°C, 30 min, N_2	A+C except W1, 3
31. 15 sec Etch	A+C except W1, 3
32. Al Evap, 10K \AA	A
33. Neg. PR, lev. 4 (metal)	A
34. Etch Al	A
35. PR strip	A
36. Sinter, 5% forming gas, 450°C, 20 min	A
37. Scribe, die attach, bond	

Notes: A means active wafers
C means control wafers

DEVICE NUMBER: P43010

DEVICE DESCRIPTION IS BIPOLAR TRANSISTOR AND WAS DEFINED 07/13/76

BY ANDERSON

AND ENTERED BY TUCK

FOR 17 WAFERS

REMARKS WAFERS ARE P-6000H (100) 0.4 x 0.3 12 ACTIVE + 5 CONTROL: NDS/2 MASK SET

NEXT STEP	NO	PROCESS	DESCRIPTION	UNIT	TIME	DATE	NUMBER WAFERS	NOTES
1	110000	CLEAN		MRT	10:51	7/14/76	17	0
2	310700	DPS ON 6000H		EN	15:58	7/14/76	17	17
3	510000	747/60% LEV. 1 3.58	MRT	9:50	7/15/76	12	0	
4	511100	ETCH HPO + 1 MIN	MRT	10:10	7/15/76	17	* 0	
5	110000	CLEAN		DLW	11:24	7/15/76	17	0
6	413400	PHOS IMP. H+O	FEZ	14: 1	7/15/76	17	0	
7	511100	ETCH 4 MIN	MRT	9:21	7/16/76	17	0	
8	310700	BASE DRIVEIN. H+O1,CHRT		10:42	7/16/76	17	17	
9	510000	747/60% LEV.2, 3.58	MRT	16:14	7/16/76	12	* 0	
10	450500	BORON IMP.H+O.NOTE INEB		9:34	7/20/76	17	0	
11	110000	CLEAN		MRT	10:49	7/20/76	17	* 0
12	310700	REP. ON DRIFTS H+OCHRT		15: 4	7/20/76	17	0	
13	311000	DRIVEIN.H+O	MRT	9: 0	7/21/76	17	13	
14	311000	H3,4,7,8,11,12,CS	MRT	9:40	7/21/76	17	13	
15	510000	747/60% LEV 3,3.58	MRT	10:57	7/21/76	17	0	
16	511100	ETCH HPO/CLD H+O	MRT	12:47	7/21/76	17	* 0	
17	999900	HOLD, NOTIFY ENG.	MRT	8:44	7/26/76	17	0	
18	110000	CLEAN		MRT	10:19	7/26/76	15	0
19	300000	H2 ANNEAL 12H, 1100C	MRT	10:54	7/26/76	17	0	
20	511100	30SEC ETCH	MRT	11:12	7/26/76	15	0	
21	999900	HOLD, NOTIFY ENG.	MRT	15:26	7/26/76	15	* 0	
22	110000	CLEAN		MRT	11:49	7/28/76	17	0
23	610400	AL EVAP. 10A	MRT	13:18	7/28/76	12	0	
24	510500	HR 100% LEV 4, 21S	MRT	15:36	7/28/76	12	0	
25	511000	AL ETCH	MRT	16: 2	7/28/76	12	0	
26	110000	3100 RESIST STRIP	MRT	9: 2	7/29/76	12	0	
27	310900	SINTER, 30 FINING CALRT		9:32	7/29/76	12	12	
28	900000	REAS RESIST ALL CONTROLS		:	/ /			
29	999900	HOLD, NOTIFY ENG.		:	/ /			

SP REN
 * 1 NOTE 1: H1-4102-03 IMPLANT B11 H5-8-04 IMPLANT B10
 * 1 H9-12-05 IMPLANT 20% B10-80% B11
 * 4 ETCH TIME 9 MIN
 * 5 ETCH AFTER PR STEI H+O2-05 CONTROLS HYPO + 1MIN
 * 11 WAFERS - TWO ACID CLEANS, NOT H2SO4, PLASMA STRIPPED (NOT. ONLY), SCRUBS
 * 10 ETCH TIME 6MIN
 * 17 WAFERS W1,3, - 11000H CLEAN, 1100 C H2 15 MIN (T9), 300 BOE - AFTER STE
 * 10 STEP 219 TUBE 9
 * 11 AFTER STEP 21 WAFERS (EXCP 1,3) SCRUBBED, ACID CLEAN AND ANNEALED T13-H2
 * 11 H2, 1000 DEGREES C 30MIN
 * 20 CH1, RES C1T-2171 C-1981 B-2011 L-1071 P-2001 N TYPE
 * 20 C1: 1-24.31 C-24.31 B-23.91 L-24.81 R-24.81 P-TYPE1
 * 26 C1: C-24.01 C4: C-25.01 C5: C-25.31 P-TYPE RES. UNIFORM ACROSS WAFERS
 * 20 HJ C1-15519A C2-14330A C3-10010H C4-29990H C5-9271H CNB 7/29/76

COPY AVAILABLE TO DDC DOES NOT PERMIT FULLY LEGIBLE PRODUCTION

APPENDIX F

Transistor Characteristics

Table F1

DC Gain Measurements on the Test Transistors
average of three devices with standard deviation

I_C ma Device	.01	.02	.05	.1	.2	.5	1	2	10	20
2A	13.5	14.1	16.2	17.7	19.3	21.5	23.2	24.6	28.3	29.7
	1.35	1.97	2.06	2.19	2.24	2.39	2.28	2.34	2.31	1.70
4A	26.0	28.0	31.2	33.8	36.3	39.4	41.6	44.5	49.9	51.1
	5.05	4.88	4.95	4.93	5.41	5.39	5.37	5.19	5.38	5.21
6A	13.6	15.5	16.9	17.6	20.0	21.9	23.6	24.9	28.5	30.0
	1.22	1.62	1.29	1.41	1.46	1.23	1.17	1.23	1.47	1.59
8A	20.3	22.8	26.5	29.1	31.6	35.4	37.7	40.6	45.7	47.6
	2.51	2.24	2.17	2.12	1.97	1.53	1.73	1.68	2.00	1.60
10A	16.9	18.5	20.7	22.4	24.2	26.3	28.0	29.3	33.5	34.7
	1.30	1.15	1.26	1.11	1.16	1.16	1.50	1.29	1.44	1.32
12A	25.7	28.3	31.4	34.4	36.6	40.0	42.4	44.8	50.1	51.3
	5.08	4.89	4.85	5.49	5.20	5.34	5.51	5.46	5.91	5.95
2B							22.8	23.4	26.5	28.0
							2.92	2.05	1.32	1.17
4B							30.1	33.1	41.8	46.0
							4.58	3.67	6.93	.907
6B							22.7	24.6	29.9	32.3
							5.75	4.82	37.7	3.45
8B							41.9	39.4	43.5	47.0
							4.45	4.06	4.82	5.53
10B							19.8	21.7	26.5	28.5
							1.91	1.56	1.48	1.41
12B							29.2	32.3	40.8	45.0
							7.50	6.30	4.29	3.10

Table F2

Leakages for Test Transistors
Average of three devices and standard deviation

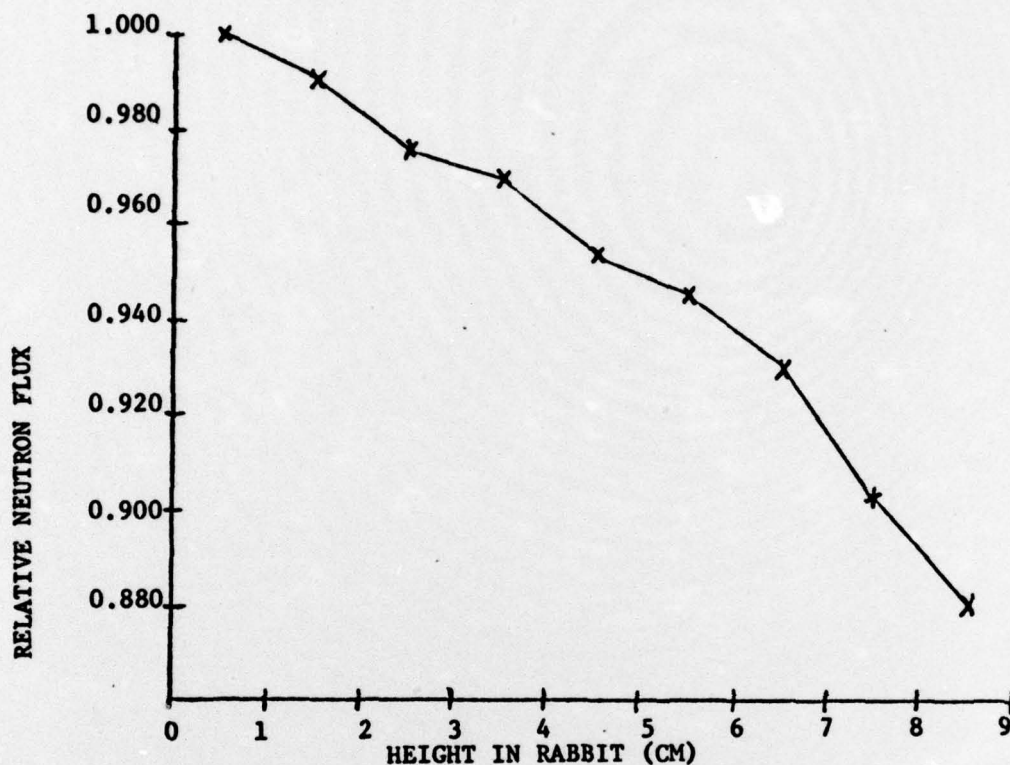
Device	I_{CBO} 10V _{CB}	I_{EBO} 3V _{BC}	I_{CEO} 10V _{CE}		I_{CBO} 10V _{CB}	I_{EBO} 3V _{EE}	I_{CEO} 10V _{CE}
2A	321 na	125pa	2.53μa	2B	23.8μa	65.4na	603μa
	141 na		1.21μa		8.46μa	110na	260μa
4A	415 na	19.5pa	3.25μa	4B	12.5μa	8.27na	544μa
	402 na	3.19pa	1.97μa		8.49μa	9.3na	178μa
6A	477 na	270pa	4.60μa	6B	6.56μa	4.02na	192μa
	240 na		2.45μa		3.69μa	4.06na	147μa
	122 na	26.4pa	3.12μa	8B	8.00μa	2.5na	675μa
	75 na	12.8pa	2.12μa		1.46μa	1.1na	123μa
10A	480 na	35pa	7.56μa	10B	3.84μa	.556na	134μa
	470 na		8.60μa		3.27μa	.306na	113μa
12A	156 na	222pa	3.26μa	12B	1.21μa	2.21na	295μa
	102 na	386pa	3.17μa		.402μa	1.53na	103μa

APPENDIX G

**Flux Information on Thermal Column
Pneumatic Tube Facility**

by D. A. Becker

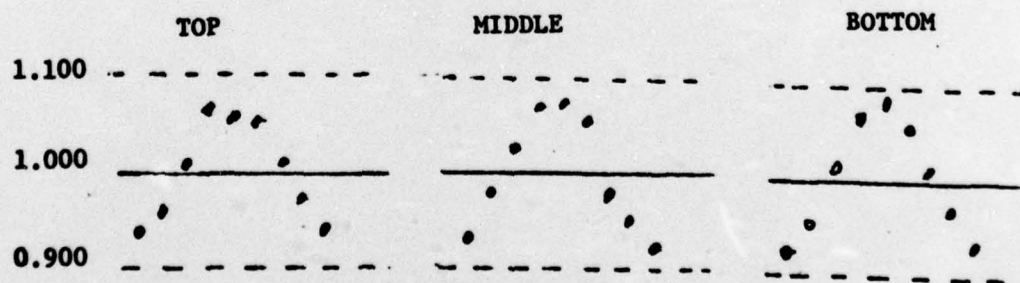
Flux Information on Thermal Column Pneumatic Tube Facility



Cu(Cd) RATIO = 3415 with center Graphite Blocks OUT

ABSOLUTE NEUTRON FLUX = $1.6 \times 10^{11} \text{ n} \cdot \text{cm}^{-2} \text{sec}^{-1}$

CIRCUMFERENTIAL FLUX DISTRIBUTION



APPENDIX H

Derivation of the Relative Damage Equation

One measure of relative effectiveness of thermal neutrons to fast neutrons in producing damage in transistors would be the ratio of the thermal neutrons bulk damage constant to the fast neutron bulk damage constant. Recall the bulk damage equation:

$$\Delta(1/\beta) = C\phi$$

Since $\Delta(1/\beta)$ is a measure of the lattice defects (Recombination Centers) in the base region, C , the bulk damage constant, must be a measure of the defects produced in the base region per neutron.

Recall that the number of reactions that occur as a result of a fast neutron irradiation is:

$$R = \Sigma \phi V$$

where R is the reactions, Σ is the Macroscopic cross-section, ϕ is the neutron fluence, and V is the volume in which the reactions occur. Recall also that the macroscopic cross-section is given by

$$\Sigma = N \sigma$$

where N is the atom density and σ is the microscopic cross section.

Thus it can be seen that the number of 1 MeV neutron reactions that occur in the base region of a transistor would be:

$$R = \sigma_{1 \text{ MeV Si}} N_{\text{Si}} \phi V$$

If we define α_1 as the defects per fast neutron (1 MeV), then the fast neutron bulk damage constant would be given by

$$C_{1 \text{ MeV}} = U_{1 \text{ MeV}} \sigma_{1 \text{ MeV}} N_{\text{Si}} V_{\text{base}}$$

for the thermal neutron case the neutron reactions take place in emitter region while the gain degrading damage is done by the lithium nucleus and the alpha particle in the base region. The geometry factor (G) derived in appendix B gives the particles doing damage in the base region per reaction in the emitter region. Thus the thermal neutron bulk damage constant would be given by:

$$C_{\text{thermal}} = (U_{\alpha} G_{\alpha} + U_{\text{Li}} G_{\text{Li}}) \sigma_{\text{thermB10}} N_{\text{B10}} V_{\text{Emitter}}$$

As long as the combined width of the emitter region and the base region is less than the path length of the lithium recoil, G_{α} and G_{Li} should remain in the same ratio. For this case it should be possible to factor out from the quantity in parenthesis an average number of defects per particle (alpha or lithium). Calling this average U_{thermal} , it follows that:

$$C_{\text{thermal}} = U_{\text{thermal}} (G_{\alpha} + G_{\text{Li}}) \sigma_{\text{thermB10}} N_{\text{B10}} V_{\text{Emitter}}$$

and

$$\frac{C_{\text{thermal}}}{C_{1 \text{ MeV}}} = \frac{U_{\text{thermal}} (G_{\alpha} + G_{\text{Li}}) \sigma_{\text{thermB10}} N_{\text{B10}} V_{\text{Emitter}}}{U_{1 \text{ MeV}} \sigma_{1 \text{ MeV}} N_{\text{Si}} V_{\text{base}}}$$

$\frac{U_{\text{thermal}}}{U_{1 \text{ MeV}}}$ was experimentally found to be approximately 1/3.3 or 0.30 as is indicated in Chapter IV. Also since the areas of the base and the emitter are equal the areas would divide out of the relative damage equation. The result is:

$$\frac{C_{\text{thermal}}}{C_{1\text{MeV}}} = \frac{0.3 (G_{\alpha} + G_{\text{Li}}) \sigma_{\text{thermB10}} N_{\text{B10}}^{\text{Emitter}} W}{\sigma_{1\text{MeVSi}} N_{\text{Si}} W_{\text{Base}}}$$

where . W is the width of the region.

VITA

Timothy Daryl Stanley was born on 2 June 1947 in Logan, Utah. He graduated from Orem High School in Orem, Utah in 1965 and attended the Brigham Young University from which he received the degree of Bachelor of Science in Physics in May of 1971. From June 1966 to June 1968 he served as a missionary for the Church of Jesus Christ of Latter-day Saints among the Navajo Indian people. He received a comission, upon graduating from college, as an officer in the USAF through the AFROTC program. He was a distinguished graduate from Operational Readiness Training for missile duty and served as a missile launch officer in the 66th Strategic Missile Squadron, Ellsworth AFB, South Dakota. While at Ellsworth AFB, he attended an extension of South Dakota State University from which he graduated with the degree of Master of Science in Economics in May of 1975. In June of 1975, he entered the School of Engineering, Air Force Institute of Technology.

Permanent address: 1363 South 800 East
Orem, Utah 84057

UNCLASSIFIED

SECURITY CLASSIFICATION OF THIS PAGE (When Data Entered)

REPORT DOCUMENTATION PAGE		READ INSTRUCTIONS BEFORE COMPLETING FORM
1. REPORT NUMBER GNE/PH/76-6	2. GOVT ACCESSION NO.	3. RECIPIENT'S CATALOG NUMBER
4. TITLE (and Subtitle) Thermal Neutron Damage in Bipolar PNP Transistors		5. TYPE OF REPORT & PERIOD COVERED MS Thesis
		6. PERFORMING ORG. REPORT NUMBER
7. AUTHOR(s) Timothy D. Stanley Captain		8. CONTRACT OR GRANT NUMBER(s)
9. PERFORMING ORGANIZATION NAME AND ADDRESS AFIT/ENP Wright-Patterson AFB OH 45433		10. PROGRAM ELEMENT, PROJECT, TASK AREA & WORK UNIT NUMBERS 62601F AD09 1132
11. CONTROLLING OFFICE NAME AND ADDRESS AFWL/ELPT Kirtland AFB NM 87117		12. REPORT DATE December 1976
		13. NUMBER OF PAGES 86
14. MONITORING AGENCY NAME & ADDRESS (if different from Controlling Office)		15. SECURITY CLASS. (of this report) Unclassified
		15a. DECLASSIFICATION/DOWNGRADING SCHEDULE
16. DISTRIBUTION STATEMENT (of this Report) Approved for public release; distribution unlimited.		
17. DISTRIBUTION STATEMENT (of the abstract entered in Block 20, if different from Report)		
18. SUPPLEMENTARY NOTES Approved for public release; IAW AFR 190-17 JERRAL F. GUESS, Captain, USAF Director of Information		
19. KEY WORDS (Continue on reverse side if necessary and identify by block number) Thermal Neutron, Bulk Damage, Displacement Damage, Gain Degradation, Transistor, Bipolar Transistor, PNP Transistor, fast Neutron, Relative effectiveness		
20. ABSTRACT (Continue on reverse side if necessary and identify by block number) An experimental test was made of the hypothesis that the source of thermal neutron damage in bipolar PNP transistors is the result of thermal neutron captures by the Boron 10 present in the emitter region of the transistors. Transistors were specifically made using three different ratios of Boron 10 to Boron 11 as the emitter dopant material, and in four different geometries. Forty-two of these specially made transistors were exposed to thermal neutron fluences as high as approximately 5×10^{15} neutrons per square centimeter 10 to the 15th power		

DD FORM 1473 1 JAN 73

EDITION OF 1 NOV 65 IS OBSOLETE

UNCLASSIFIED

SECURITY CLASSIFICATION OF THIS PAGE (When Data Entered)

UNCLASSIFIED

SECURITY CLASSIFICATION OF THIS PAGE(When Data Entered)

In each case the damage observed corresponded to the fraction of Boron 10 to total boron used as the emitter dopant material, thus confirming the hypothesized damage mechanism. The dependence of the collector current, thermal neutron fluence, and emitter-base geometry on the observed gain degradation also indicated that bulk damage is responsible for thermal neutron damage in PNP transistors. Some devices were also irradiated in a fast neutron environment. Fast neutrons were found to be approximately one hundred times more effective than thermal neutrons in producing damage in the devices that use a naturally occurring ratio of Boron 10 to Boron 11 in the emitter. Formulas were developed to calculate the fraction of lithium atoms and alpha particles generated in the emitter that do damage in the base, and to calculate the relative effectiveness of fast and thermal neutrons in producing damage in PNP transistors where the combined thickness of the emitter and base regions is less than the path length of a .88 MeV lithium nucleus in silicon.

UNCLASSIFIED

SECURITY CLASSIFICATION OF THIS PAGE(When Data Entered)